Phase Change Solvents in Carbon Dioxide Capture

Tytti Lahti

Porvoo, 8.4.2014

OULUN YLIOPISTO
UNIVERSITY of OULU

FACULTY OF TECHNOLOGY

PHASE CHANGE SOLVENTS IN CARBON DIOXIDE CAPTURE

Tytti Lahti

Master's thesis
Degree programme in environmental engineering
April 2014

ABSTRACT FOR THESIS

University of Oulu Faculty of Technology

Degree Programme (Bachelor's Thesis, Master's Thesis) Environmental engineering	Major Subject (Licentiate Thesis)
Author Lahti Tytti	Thesis Supervisor Keiski Riitta, Prof.

Title of Thesis Phase change solvents in carbon dioxide capture

Major Subject Industrial Environmental Engineering and Biotechnology	Type of Thesis Master's thesis	Submission Date April 2014	Number of Pages 97 + 6 p.

Abstract

New technologies are under study to find solutions to slow down global warming and climate change. One option is the capture of the greenhouse gas carbon dioxide from industrial outlet gases and storage of it. However, the most commonly applied method of using amine as a solvent has the problem of high energy consumption in the solvent regeneration. The aim of this thesis was to study phase change solvents as an alternative to decrease the energy consumption of the CO_2 capture process. The phase change solvents have the property of forming a third phase for specific carbon dioxide loading, temperature or pressure conditions. The phase can be either liquid or solid. In this thesis an aqueous solvent blend of 2-(diethylamino)ethanol (DEEA) and (3-(methylamino)propylamine (MAPA) is further investigated mainly as a literature survey. When loaded in an absorber with carbon dioxide it forms two immiscible liquid phases. The upper phase with lower density consists mainly of DEEA and the lower heavy phase consists of MAPA and carbon dioxide. The loaded solvent is led to a separator where the two phases are separated. The system saves energy as only the loaded heavy phase is led to a stripper for regeneration. The lean solvent recycled from the stripper is taken to a mixer where it is mixed with the light phase from the separator. After this the mixture is fed back to the absorber. Relatively low temperature or elevated pressure for the solvent regeneration can also be used. The energy efficiency presented as the reboiler heat duty per amount of absorbed carbon dioxide is better for the blend than for reference aqueous solvent of monoethanolamine (MEA). Loading is an important factor as it tells the amount of amine needed to capture the wanted amount of carbon dioxide. The loading depends on the partial pressure of carbon dioxide, the change in temperature, the type of amine, the amine concentration in the solution and the nature and concentration of other components in the solution. As the energy efficiency and other properties of DEEA and MAPA blend were found promising based on the literature survey, the process was also studied for an industrial scale. The required solvent flow rate was calculated to capture carbon dioxide. Flow rate and composition of flue gas of a coal fired power plant of 565 MW was used. The solvent flow rate was found to be lower than for activated aqueous methyldiethanolamine (MDEA) but higher than for MEA with the same loading. Also a gravity settler was dimensioned for the system based on the viscosities and densities of loaded solvent. The density and viscosity of the heavy phase are high, which makes the separation of the two phases very slow. Due to a long settling time the dimensions of the decanter were calculated to be too big to be feasible. However, according to the literature the settling time may be shortened by using coalescers, by increasing temperature or with another separation technique like centrifugation. Finally, the amount of amine in the stripper CO_2 outlet was calculated to estimate the CO_2 purity. It can be removed and recycled back to the process. Simplifications were made for the calculations. Only limited amount of data from laboratory, pilot and simulation tests was available for the scale-up. No practical experiences of an industrial capture system with DEEA + MAPA exist. Because of these the validity of the results is uncertain. Nevertheless, those give an idea of the problems that might come along and directions for further investigations.

Additional Information

TIIVISTELMÄ OPINNÄYTETYÖSTÄ

Oulun yliopisto Teknillinen tiedekunta

Koulutusohjelma (kandidaatintyö, diplomityö) Ympäristötekniikka	Pääaineopintojen ala (lisensiaatintyö)
Tekijä Lahti, Tytti	Työn ohjaaja yliopistolla Keiski, Riitta, prof.

Työn nimi Hiilidioksidin talteenotto faasiaan muuttavilla liuottimilla

Opintosuunta Teollisuuden ympäristö- ja biotekniikka	Työn laji Diplomityö	Aika Huhtikuu 2014	Sivumäärä 97 + 6 s.

Tiivistelmä

Uusia teknologioita tutkitaan kasvihuoneilmiön ja ilmaston lämpenemisen estämiseksi. Yksi vaihtoehto on tärkeimmän kasvihuonekaasun hiilidioksidin talteenotto teollisuuden päästöistä ja sen varastointi. Amiiniliuotinta käyttävä yleisin talteenottomenetelmä kuluttaa kuitenkin paljon energiaa liuottimen regeneroinnissa. Tämän diplomityön tavoitteena oli tutkia faasiaan muuttavien liuottimien käyttöä hiilidioksidin talteenottoprosessissa energiakulutuksen vähentämiseksi. Tietyllä hiilidioksidin liukoisuudella tai tietyssä lämpötilassa ja paineessa liuottimet muodostavat kolmannen faasin, joka on joko nestemäinen tai kiinteä faasi. Tässä diplomityössä keskitytään faasiaan muuttavaan 2-(dietyyliamino)etanoli (DEEA) + 3-(metyyliamino)propyyliamiini (MAPA) + vesi -seokseen. Absorboituaan hiilidioksidia se muodostaa neste-nestefaasin. Ylempi faasi, jolla on pienempi tiheys, koostuu enimmäkseen DEEA:sta ja alempi raskas faasi MAPA:sta ja hiilidioksidista. Liuotin ja absorboitunut hiilidioksidi johdetaan absorberista erottimeen, jossa kaksi nestefaasia erotetaan toisistaan. Systeemin energiansäästö perustuu siihen, että ainoastaan alempi faasi johdetaan stripperiin regeneroitumaan. Stripperistä saatava regeneroitu liuotin johdetaan sekoittimeen, missä se sekoitetaan erottimesta tulevan kevyen faasin kanssa. Sieltä liuotin johdetaan takaisin absorberiin. Liuotin voidaan myös regeneroida alemmassa lämpötilassa tai korkeammassa paineessa kuin perinteisesti hiilidioksidin talteenotossa käytetyt amiinit. Energiatehokkuus talteen otettua hiilidioksidikiloa kohti on parempi kuin vertailussa käytetyllä monoetanoliamiiniliuottimella (MEA). Energiatehokkuuden lisäksi absorboidun hiilidioksidin ja amiinin moolisuhde on tärkeä tekijä, sillä se kertoo paljonko amiinia tarvitaan tietyn hiilidioksidimäärän absorboimiseen. Suhteeseen vaikuttaa hiilidioksidin osapaine, lämpötila, käytetty amiini, amiinipitoisuus seoksessa ja muut komponentit sekä niiden määrä. Koska kirjallisuusselvityksen mukaan DEEA + MAPA -systeemin energiatehokkuus ja muut ominaisuudet vaikuttivat lupaavilta, tässä diplomityössä käsiteltiin talteenottoprosessia myös teollisuusmittakaavassa. Tietyn hiilidioksidimäärän talteenottoon tarvittava liuottimen minimivirtaus laskettiin. Laskuissa käytettiin 565 MW:n voimalaitoksen savukaasun virtausnopeutta ja koostumusta. Liuottimen syötön määrä osoittautui pienemmäksi kuin verratun aktivoidun metyylidietanoliamiiniliuottimen (MDEA) mutta suuremmaksi kuin MEA:n. Myös erotin mitoitettiin systeemille hiilidioksidia absorboineen liuottimen viskositeetin ja tiheyden perusteella. Raskaan faasin viskositeetti ja tiheys ovat korkeat, mikä tekee kahden faasin erottumisen hyvin hitaaksi. Pitkän erottumisajan vuoksi erottimen mitat olivat liian suuret ollakseen toteutettavissa. Erottumisaikaa voitaisiin kirjallisuuden mukaan lyhentää edistämällä pisaroitumista, nostamalla lämpötilaa tai tehokkaammalla erotusmenetelmällä, kuten sentrifugoimalla. Lopuksi on arvioitu stripperistä ulostulevan hiilidioksidin mukana poistuvan amiinin määrä. Amiini voidaan erottaa ja palauttaa prosessiin. Laboratorio-, pilotti- ja simulointikokeiden tuloksia oli kirjallisuudessa saatavilla hyvin rajoitetusti. Käytännön kokeita teollisen mittakaavan talteenottosysteemille DEEA + MAPA -liuotinta käyttäen ei ole toteutettu vielä lainkaan. Laskuissa jouduttiin tekemään yksinkertaistuksia ja oletuksia, minkä vuoksi tulosten oikeellisuudesta on mahdoton antaa varmuutta. Joka tapauksessa tulokset tuovat esille mahdollisia ongelmia, joita prosessissa voi ilmetä erityisesti siirryttäessä suurempiin laitoksiin. Tulokset antavat myös suuntaa jatkotutkimuksille.

Muita tietoja

PREFACE

This thesis was carried out as a part of the CLEEN's Carbon Capture and Storage Program (CCSP), which is funded by Tekes – the Finnish Funding Agency for Technology and Innovation. I'm grateful for having this opportunity to participate the project. The work for this thesis was performed at Neste Jacobs Oy in the Competence Center Technology and Process.

The advisors for my thesis were Kari Keskinen, Timo Nyman, Rauli Koskinen and Esa Turpeinen who I would like to thank for the feedback and assistance. I would also like to thank Jussi Laitio for partisipating the meetings and giving directions and Riitta Keiski for being my supervisor. In addition I thank Petri Uusi-Kyyny for performing the experiments I needed for my thesis.

Finally, I would like to acknowledge my family for all the support during this project and throughout my studies, especially my mother who I have always looked up to. I am also grateful for my friends and the student organisations I have been member of as they have made my student life the best.

In Porvoo, 4th of April , 2014

Tytti Lahti

TABLE OF CONTENTS

LIST OF ABBREVIATIONS AND SYMBOLS

Abbreviations

CO_2	Carbon dioxide
$CO_{2(g)}$	Carbon dioxide in gas phase
$CO_{2(l)}$	Carbon dioxide in liquid phase
CO_3^{2-}	Carbonate ion
DEEA	2-(diethylamino)ethanol
$DEEAH^+$	Protonated 2-(diethylamino)ethanol
Eq.	Equation
$H^+MAPACOO_p^-$	Protonated 3-(methylamino)propylamine carbamate (primary)
$H^+MAPACOO_s^-$	Protonated 3-(methylamino)propylamine carbamate (secondary)
HCO_3^-	Bicarbonate ion
H_2O	Water
H_3O^+	Hydronium ion
HP	Heavy phase
H_2S	Hydrogen sulphide

LP	Light phase
MAPA	3-(methylamino)propylamine
MEA	Monoethanolamine
$MAPA(CO_2^-)_2$	3-(methylamino)propylamine dicarbamate
$MAPACOO_p^-$	3-(methylamino)propylamine carbamate (primary)
$MAPACOO_s^-$	3-(methylamino)propylamine carbamate (secondary)
$MAPAH^+$	Protonated 3-(methylamino)propylamine
$MAPAH^{2+}$	Di-protonated 3-(methylamino)propylamine
OH^-	Hydroxide ion
$R_1R_2NCOO^-$	Primary amine carbamate ion
R_1R_2NH	Alkanolamine
$R_1R_2NH_2^+$	Protonated amine
R_3N	Amine
R_3NH^+	Protonated amine

Symbols

A	Cross-sectional surface area of a cylinder [m^2]
A_c	Flow area of the continuous phase [m^2]

A_{HP}	Cross-sectional surface area of the heavy phase [m^2]
A_{i}	Area of the liquid-liquid interface [m^2]
A_{k}	Area of the isosceles triangle [m^2]
A_{LP}	Cross-sectional surface area of light phase [m^2]
A_{S}	Area of a sector [m^2]
d	Droplet diameter [m]
d_{min}	Minimum diameter of a settling droplet [m]
D	Diameter of the gravity settler vessel [m]
D_{h}	Hydraulic diameter [m]
g	Gravitational acceleration, 9,81 $\mathrm{m/s}^2$
H_{c}	Height of the continuous phase [m]
H_{i}	Height of the liquid-liquid interface from the middle of the vessel [m]
H_{HP}	Height of the heavy phase [m]
H_{LP}	Height of light phase [m]
L	Length of the gravity settler vessel [m]
L_{i}	Width of the liquid-liquid interface [m]
L/G	Liquid to gas ratio [$\mathrm{kg/m}^3$]

m_i	Mass flow rate of the component *i* [kg/h]
$m_{\mathrm{liquid,1}}$	Mass flow of the liquid 1 [kg/h]
$m_{\mathrm{liquid,2}}$	Mass flow of the liquid 2 [kg/h]
m_{MAPA}	Mass flow of MAPA [kg/h]
m_{OUT}	Outlet flow of loaded solvent from the absorber [kg/h]
m_{solvent}	Total mass flow of the solvent feed [kg/h]
M_i	Molar mass of the component *i* [g/mol]
M_{TOT}	Average molar mass of a mixture [mol]
n_i	Molar amount of a substance *i* [mol]
N_{amine}	Amine molar flow [mol/h]
N_{CO2}	CO_2 molar flow [mol/h]
N_i	Molar flow of the component *i* [mol/h]
p_i	Partial pressure of the component *i* [kPa]
P	Total pressure [kPa]
Q_{c}	Volumetric flow rate of the continuous phase [m^3/s]
$Q_{\mathrm{gas,1}}$	Volumetric flow rate of the gas 1 [m^3/h]
$Q_{\mathrm{gas,2}}$	Volumetric flow rate of the gas 2 [m^3/h]
Q_{HP}	Volumetric flow rate of the heavy phase [m^3/h]

Q_i	Volumetric flow rate of the component i [m^3/h]
Q_{LP}	Volumetric flow rate of the light phase [m^3/h]
r	Separator radius $r=D/2$ [m]
S_{c}	Arc of the continuous phase cross-sectional area [m]
S_{LP}	Arc of the light phase cross-sectional area [m]
S_{HP}	Arc of the heavy phase cross-sectional area [m]
t_1	Final temperature [°C]
t_0	Initial temperature [°C]
t_{c}	Residence time of the continuous phase [s]
t_{d}	Time for the drop to rise or fall [s]
v_{c}	Continuous phase cross-flow velocity [m/s]
v_{d}	Settling terminal velocity of the dispersed phase droplets with the diameter d [m/s]
v_{i}	Continuous phase overflow velocity [m/s]
V	Volume of a separator vessel [m^3]
V_1	Volume of the phase 1 [m^3]
V_2	Volume of the phase 2 [m^3]
V_{c}	Volume of the continuous phase [m^3]

V_{HP}	Volume of the heavy phase [m^3]
V_{LP}	Volume of the light phase [m^3]
w_1	Mass ratio of the phase 1
w_i	Mass ratio of the component *i*
w_{TOT}	Total mass ratio
x_i	Molar ratio of the component *i*

Greek symbols

α	Loading of CO_2 in to amine [mol/mol]
β	Volumetric temperature expansion coefficient (m^3/m^3°C)
μ_c	Viscosity of the continuous phase [Ns/m^2]
μ_{HP}	Viscosity of the heavy phase [Ns/m^2]
μ_{LP}	Viscosity of the light phase [Ns/m^2]
ρ_1	Density of the phase 1 [kg/m^3]
ρ_2	Density of phase 2 [kg/m^3]
ρ_{0T}	Initial density [kg/m^3]
ρ_{1T}	Final density when temperature is changed [kg/m^3]

ρ_{c}	Density of the continuous phase [kg/m^3]
ρ_{d}	Density of the dispersed phase [kg/m^3]
ρ_{HP}	Density of the heavy phase [kg/m^3]
ρ_i	Density of the component *i* [kg/m^3]
ρ_{LP}	Density of the light phase [kg/m^3]
ρ_{TOT}	Total density of the mixture [kg/m^3]

1 INTRODUCTION

After the industrialisation the consumption of fossil fuels has increased massively releasing an enormous amount of greenhouse gases into the atmosphere. These include carbon dioxide that is the main component causing global warming and climate change. Its amount in the atmosphere is increasing at an accelerating rate.

Fuels from renewable raw materials are under development to replace fossil fuels but to slow down global warming more urgent solutions are needed. To reduce the carbon dioxide emissions, gas purification methods have been developed. The captured CO_2 is compressed and stored underground or into sea bottom.

Carbon dioxide is mostly captured with a chemical solvent. Solvent absorption is the most developed technology and it has been implemented and used commercially for tens of years already in the oil and gas industry. However, the most applied processes that use amines as solvents have the problem of high energy consumption in the regeneration.

The aim of this thesis is to study solutions to decrease the energy consumption and costs of the CO_2 capture process. As regeneration of the solvent is often the part of the process having the greatest energy demand, it is natural to focus on new solvents with the property of low requirement for regeneration energy. However, there are many other properties like CO_2 absorption capacity and rate of reaction that should be also taken into consideration. Solvents have been found to have different characteristics and the studies are now focusing on solvent mixtures with mixed properties to find an optimal solvent for CO_2 capture. One solvent under study is the mixture of 2-(diethylamino)ethanol (DEEA) and 3-(methylamino)propylamine (MAPA). When it comes to decreasing the energy consumption, it has the advantage of forming two liquid phases when loaded with CO_2. Only the CO_2 rich phase is taken to regeneration, which is assumed to have a remarkable improvement to the energy requirements of the process. It has also a positive effect on investment and operating costs. Also other phase changing solvents are investigated in this thesis but the main focus is in the method of DEEA and MAPA.

The studies in the literature are giving results mostly from laboratory tests and finding a proper model to fit with the behaviour of the system. Although the results are promising the laboratory scale can differ a lot from the system for a commercial process. Especially interesting is the property of high viscosity of the CO_2 rich phase, which might cause problems in the commercial scale. Viscosities and densities of the loaded aqueous DEEA + MAPA solvent are used to dimension a gravity settler that separates the two phases. A preliminary flow rate scale-up for the capture unit of a coal fired power plant of 565 MW is made.

2 POST-COMBUSTION FOR CO_2 CAPTURE

Post-combustion with a solvent is the main method of capturing greenhouse gases like carbon dioxide from the flue gas of a power plant or factory emission. Retrofitting is often easily implemented and integrated into the existing processes as it does not require any modifications in the core plant process. The operation of a post-combustion capture process does not either affect the core operations. (Onarheim 2012.) However, as an example the capturing and compression of CO_2 with current methods increase the fuel need of a coal-fired carbon capture plant with 25-40%. The capturing itself and compression of the captured CO_2 are causing 80% of the costs of the process when 20% comes from transportation, monitoring and injection. (Zubeir et al. 2013.)

Different chemical solvents are the most developed methods for absorption-desorption (Wang et al. 2011). Whether the separation method is based on physical or chemical absorption of CO_2 is often chosen depending on the partial pressure of CO_2 in the gas stream. Chemical absorption is preferred when the partial pressure is not high. (Zubeir et al. 2013.) The different chemical solutions require different process conditions, which bring opportunities for energy and process optimization. (Onarheim 2012.)

The carbon dioxide absorption takes place in columns where CO_2 transfers from gas to liquid during a counter current flow. The flue gas enters the absorber at the bottom, whereas the solvent feed is at the top of the column. The contact area between phases is maximized for example with a packed bed. The solvent loaded with CO_2 then flows into a stripper, where the solvent is heated typically with steam. CO_2 desorbs and can be recovered, cooled and compressed. The stripped solvent can be recycled back to the absorber. (Herzog et al. 2009.)

Alternatives for post-combustion would be the oxy-combustion capture, where the power plant uses high purity oxygen stream for the combustion of coal. This eliminates the major component nitrogen from the flue gas, which makes the process of capturing CO_2 easier. However, the oxygen production is the largest cost of the capture process. The other alternative, the pre-combustion capture can be used in integrated coal gasification combined cycle (IGCC) plants, where CO_2 is removed during the process.

This alternative is very affordable, but the plant itself is expensive to run. (Herzog et al. 2009.)

2.1 Selection of the method

The requirements for the capturing process can be very different depending on the process the combustion is retrofitted, the composition of the gas stream and the purpose of use of CO_2. Listed by Onarheim (2012) the factors to begin with when choosing the most appropriate CO_2 capture technology are:

- partial pressure of CO_2 in the gas stream,
- extent of CO_2 recovery required,
- sensitivity to impurities (acid gases, dust/particulate matter, nitrogen, sulphur, heavy metals),
- CO_2 purity,
- capital and operational expenses (CAPEX and OPEX),
- environmental concerns.

The primary driver for research and development is to decrease the high energy consumption process linked to vapour-liquid equilibrium (VLE) properties. Also the compression of CO_2 and pre- and post-conditioning the flue gases linked to degradation issues are to be taken into consideration. (Raynal et al. 2011.) Right after heat duty, the compression of CO_2 is the second largest contributor to the net efficiency loss of the power plant. Also the instrumentation including pumps, blowers, CO_2 compressor and additional cooling water pumps and their electrical duty and the amount of cooling water needed in both capture and compression are to be considered. (Liebenthal et al. 2011b.) At the same time as the energy consumption is reduced it has an effect on investment costs that already form a great deal of the overall costs of CO_2 capturing (Raynal et al. 2011).

2.2 Solvent requirements

In practise the solvent is chosen based on the most optimal combination of different qualities for the situation. However, when new solvents are studied there can be certain properties that the ideal solvent would have. For example, the solvent should be selective for CO_2. In post-combustion of flue gases it means that carbon dioxide dissolves into the solvent more readily than nitrogen does. Also the capacity of how much the solvents can absorb CO_2 is important as otherwise the industrial amounts of CO_2 would require excessive solvent circulation. Organic solvents have good CO_2 solubility. In near atmospheric pressures like in coal-fired power plants it is preferred to use aqueous solutions that react reversibly with dissolved CO_2. CO_2 is absorbed in the absorber and the release of it in the stripper requires higher temperature. (Herzog et al. 2009.)

Degradation of the solvent causes corrosion, foaming and unwanted emissions. The solvent must be reclaimed or the lost solvent replaced, which increases the operational costs. (Raynal et al. 2011.) Chemical solvents have a concentration of 10% to 50% by weight in aqueous solutions. By optimizing concentrations the CO_2 capacity can be increased and the viscosity and risk of corrosion decreased. (Mustonen 2013.)

Capital costs of absorption decrease when the rates of CO_2 absorption and desorption increase. When transfer rates are high the gas to liquid exposure time can be shorter and thus the absorbers and strippers smaller. This decreases energy need, because the blower and the pump work for the liquid transfer is needed less. It reduces the operational costs. The main operational costs however come from heating the steam needed for warming the loaded solvent. (Herzog et al. 2009.)

Following list gathers some properties that an ideal solvent should have (Mustonen 2013: 17., Onarheim 2012: 7., Yeh & Bai 1999):

- high reactivity with respect to CO_2 (fast CO_2 absorption kinetics) that reduce the capital investment by enabling the implementation of a smaller absorber size that further reduces circulation of solvent flow rates,

- low heat of CO_2 absorption or low regeneration cost if heat of reaction with CO_2 is high,

- high inherent CO_2 capacity per weight of solvent, which results in lower solvent flow rates,

- high thermal stability and reduced solvent degradation under the operating conditions of the columns, which will reduce the solvent loss,

- low environmental impact, for which non-corrosive, non-volatile, non-toxic and non-hazardous behaviour are to be considered,

- low vapour pressure and low viscosity,

- low solvent cost.

When identifying new amine solvents the focus has been mainly on the enthalpy of the reaction and on kinetics, that are chosen based on a qualitative approach. However, many new studies have a quantitative approach of comparing new solvents with the conventional solvent mass fraction of 30% monoethanolamine (MEA) cost repartition. (Raynal et al. 2011.)

2.3 Amine absorption

Absorption is the most important operation of gas purification processes. Processes can be physical, reversible or irreversible based on the behaviour. Physical solutions do not react chemically with the components in the gas stream but physically dissolve the specific acid gases. Components are then stripped by reducing the pressure, which requires no heat. When the solution reacts chemically and reversibly, the solvent reacts with the gaseous component and forms a loosely bound product. The product has certain vapour pressure of the absorbate that increases with temperature, which enables reversible reaction. In absorption with irreversible reaction the product cannot readily be decomposed to release the absorbed component. (Herzog et al. 2009.)

Carbon dioxide capture by chemical absorption with aqueous amine and stripping of it is technology that is well understood and commonly used. Amines are organic derivatives of ammonia in which one or more of the hydrogen atoms have been replaced by an alkyl or aromatic group (Herzog et al. 2009). Amines react rapidly, selectively and reversibly with CO_2 and they are also quite non-volatile and affordable (Rochelle 2009).

Weakly basic amines react with acid gases converting them into ions and thus trapping them into the liquid phase. It is assumed that hydrogen bonding between amine and water is the mechanism for CO_2 hydration catalysis. It makes the H-O bond weaker and the nucleophilic reactivity of water towards CO_2 increases, which is presented in Equation (1). Free hydroxide is never actually formed (Donaldson & Nguyen 1980).

$$R_3N + H\text{-}O\text{-}H + CO_2 \rightarrow R_3NH^+ + HCO_3^- \tag{1}$$

where R_3N is an alkanolamine.

Alkanolamines have been preferred for long as they have an alcohol group that reduces considerably the vapour pressure of the amine, which decreases contamination risk of the treated gas by amine. Even at high amine concentration, an alcohol group increases the solubility of the amine in water, and keeps the dielectric constant of the solvent high. In addition, alcohol groups allow tuning of the basicity of the amine, and thus its reactivity, in order to be in adequacy with the acidity of the gas. (Raynal et al. 2011.)

Most used chemical in the capture process is the primary alkanolamine monoethanolamine that is a non-selective solvent removing acid gases such as CO_2 and hydrogen sulphide H_2S. Concerns about its volatilisation, degradation and corrosion have kept the solvent concentration quite low. This has led to large equipment sizes and solvent regeneration costs as it requires lots of energy. (Herzog et al. 2009.) To heat and condensate the water needed for MEA-based processes is estimated to increase the cost of energy by around 80-85% and decrease the power plant efficiency by around 30% (Perry et al. 2012).

There are also many other amines and their blends that are studied for better properties and energy savings, such as secondary amines like diethanolamine (DEA) and di-isopropanolamine (DIPA); tertiary amine methyldiethanolamine (MDEA) with different activators; and sterically hindered amines like 2-amino-2-methyl-1-propanol (AMP) (Sartori & Savage 1983., Kohl & Nielsen 1997., Rochelle 2009., Barzagli et al. 2010., Mustonen 2013).

2.3.1 Primary and secondary amines as solvents

Primary and secondary amines have fast reaction rates. The heat of reaction is high and thus also high heat for reversion is needed. (Arshad et al. 2013b.) Primary and secondary amines can react with dissolved CO_2 to form carbamic acid. Depending upon its acidity, it may then give up a proton to the second amine molecule forming a stable carbamate. (Puxty et al. 2009.)

The loading of CO_2 for primary and secondary amines is 0.5 mol of CO_2 per mol of alkalinity. This is when there occurs a reaction only for carbamate formation. (Sartori & Savage 1983.) However, in the study of Ciftja et al. (2013b) aqueous solutions of diamines consisting of primary ethylenediamine, primary/secondary 3-(methylamino)propylamine and secondary piperazine were found to have higher CO_2 absorption capacity than other mainly studied amines, due to carbamate hydrolysis that generates free amine to react with additional CO_2.

2.3.2 Tertiary amines as solvents

When searching solvents that have lower energy requirements, reactive absorption of CO_2 with tertiary amines solutions has been considered. Since tertiary amines have no hydrogen atom attached to the nitrogen atom, as in case of primary and secondary amines, the carbamation reaction cannot take place (Donaldson & Nguyen 1980). The reaction forms bicarbonates, which have lower heat of reaction than carbamates (Monteiro et al. 2013). The reaction is also slower, but selectivity higher. As the heat of reaction is low also the heat that is required for the amine regeneration is low, which means less energy is needed for the process (Arshad et al. 2013c., Liebenthal et al. 2013).

Tertiary amines such as MDEA and DEEA have high loading capacity of around 1.0 mol of CO_2 per mol of alkalinity, which means that they have a good potential for bulk removal of CO_2 (Ciftja et al. 2013c). However, tertiary amines have low reaction rates with CO_2. Tertiary amines also need to be in contact with water in order to react with carbon dioxide (Aleixo et al. 2011). To enhance CO_2 capture an activator with a faster absorption rate is needed. The activator can be primary or secondary amine or a totally different chemical. (Kim & Svendsen 2007.)

3 PHASE CHANGE SOLVENTS

In addition to basic amine absorbent processes a carbon dioxide capture approach called the phase change system has been developed. It is using a solvent with thermodynamic properties forming a third phase for specific CO_2 loading, temperature or pressure conditions. The third phase makes it possible to significantly decrease the energy requirements for the regeneration in the stripper. The phase can be either liquid or solid. (Raynal et al. 2011.) Chilled ammonia process forming a solid phase is already widely studied and under development by Alstom (Alstom 2012). Also deep eutectic solvents and aminosilicones show potential (Zubeir et al. 2013., Perry et al. 2012). The studied phase change solvents forming two liquid phases are for example DMX™ developed by IFPEN and tested in the EU OCTAVIUS project (Raynal et al. 2011., Aleixo et al. 2011) and DEEA + MAPA system in the EU project iCap, the process that is ready for an industrial prototype (Arshad et al. 2013b., Liebenthal et al. 2013., Ciftja et al. 2013c). The potential of the solvent mixture of DEEA + MAPA with good absorption capacity, chemical stability and energy requirement reduction makes it an interesting option and is thus dealt more in detail in this work.

3.1 Liquid-liquid solvents

3.1.1 Solvent mixture DEEA + MAPA

2-(Diethylamino)ethanol (DEEA) (Figure 1) is an attractive absorbent for CO_2 removal from gaseous streams as it can be prepared from renewable sources and it gives low heat of absorption. Tertiary amines contain two ethyl groups replacing the hydrogen atoms of the amino groups in MEA. DEEA forms from the reaction of diethylamine obtained from ethanol and ethylene oxide obtained from the oxidation of ethylene which is in turn prepared by dehydrating ethanol. The raw material ethanol can be prepared from renewable resources. (Konduru et al. 2010.)

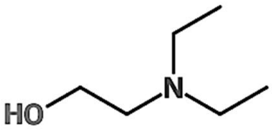

Figure 1. Chemical structure of DEEA.

3-(Methylamino)propylamine (MAPA) (Figure 2) is a diamine with one primary and one secondary amine group in its structure. This enables high CO_2 absorption capacity and high reaction rate. (Ciftja et al. 2013c.) The high basicity of MAPA results in carbamate formation instantly after CO_2 is introduced into the solution. In contrary to DEEA, MAPA is difficult to regenerate as CO_2 loading remains high even at higher temperatures, so more energy is consumed in stripping conditions. This is why MAPA is not very attractive as a single absorbent. (Kim 2009., Ciftja et al. 2013c.)

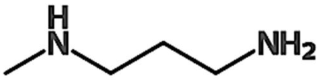

Figure 2. Chemical structure of MAPA.

For the demixing process the combination of 2-(diethylamino)ethanol and 3-(methylamino) propylamine is a promising alternative for absorption of CO_2. Although the study of Arshad et al. (2013b) shows that the amine mixture has a relatively lower CO_2 absorption capacity than its constituent amines used as single solvents, it has its advantages. The CO_2 loading capacity is higher than with traditional MEA, equilibrium temperature sensitivity is high, energy requirement for regeneration is low and reaction rate is relatively fast. (Ciftja et al. 2013c.) Hartono et al. (2013) observed also that in the presence of each other the volatility of both is reduced. This helps to retain good liquid load in the absorber.

The system forms two liquid phases under certain conditions after absorption. The volume ratio of the two phases depends on the total CO_2 loading in the mixture. The higher the CO_2 loading is the more volume will be in the lower heavy phase. (Arshad et al. 2013b.) The heavy phase is rich with CO_2 and MAPA and the light phase is rich in DEEA and lean in CO_2. However, with the increase in CO_2 loading, more DEEA shifts to the lower phase. (Ciftja et al. 2013c., Arshad et al. 2013b.) Tertiary amine DEEA is preferably stripped, which can potentially lower the energy demand of the reboiler. Only the heavy phase is taken to the stripper for the regeneration. It has high viscosity that has to be taken in to consideration in transition. The separated light phase that is lean in CO_2 is mixed with the regenerated heavy phase and is recycled then back to the absorber. (Liebenthal et al. 2013.) Arshad et al. (2011) also noticed that amine solutions with high concentrations were foaming when stirred. These are to be taken into consideration in the design.

In the study of Liebenthal et al. (2013) the pressure of the heavy phase was measured after the separation of the two phases. The total pressure of the heavy phase was a lot higher than with the benchmark MEA of mass fraction 30%. From this follows that the requirement for the energy decreases for the same regeneration as for MEA the regeneration could be performed at lower temperatures and at elevated pressures, which in turn reduces the need of energy for CO_2 compression. Because of the higher pressure in the stripper the column size can be diminished. On the other hand, the study of Liebenthal shows that the lower the pressure the lower the heat duty of the stripper is, which sets another challenge in finding the optimal conditions for the system.

According to the study of Brakstad et al. (2013) MAPA is biodegradable both in fresh water and seawater. However, DEEA is biodegradable only in freshwater, but it doesn’t reach the lowest acceptable value for release in the marine environment. The mixture does not reach the value either. (Brakstad et al. 2013., Eide-Haugmo et al. 2009.) According to the OSPAR system for environmental classification the chemicals are classified as “acceptable” (Brakstad et al. 2013).

3.1.2 DMX™

DMX™ is a process developed by IFP Energies Nouvelles. It is based on a special solvent that forms two immiscible phases at certain temperature and CO_2 loading. The other phase is free of CO_2 and highly concentrated with amine and the other phase is rich with CO_2 and water. Primary, secondary and tertiary amines can be used as the solvent. The solvent has very good CO_2 absorption capacity, very good stability and thus a low degradation rate, low corrosion and fast separation of the two phases. The easy separation of the two phases decreases the mass flow of regeneration as only the heavy phase is taken to the stripper. This leads to reduction in energy consumption. Reboiler duty of 2.1 GJ/t CO_2 can be reached, which is significantly lower than the 3.7 GJ/t CO_2 of the 30% mass fraction of MEA reference process. After regeneration it is mixed with the lean phase and fed back to the absorber. As DMX™-1 solvent showed low corrosiveness in experiments, savings can also be made in construction materials and by avoiding the need of corrosion inhibitors. (Raynal et al. 2011.)

3.1.3 Solvent mixture BDA-DEEA

The mixture of 1,4-butanediamine (BDA) and 2-(diethylamino)-ethanol DEEA form two liquid phases when loaded with carbon dioxide. According to the study of Xu et al. (2013) the optimal concentration is 2 M of BDA and 4 M of DEEA in an aqueous blend. The cyclic loading is 46% higher and cyclic efficiency 11% higher than that of 5 M MEA. The formation of two phases is caused by the limited solubility of DEEA into the reaction products of BDA and CO_2 as the reaction rate of BDA is faster. At higher loadings DEEA reacts with CO_2 of the products that have transferred to the lower phase. The products with BDA in the upper phase are mainly carbamates as in the lower phase there are also fractions of BDA and bicarbamates. (Xu et al. 2013.)

3.1.4 Thermophilic biphasic solvents

The thermophilic biphasic solvents (TBS) are lipophilic amines that exhibit a thermomorphic phase transition when heated, which improves desorption at temperatures well below the solvent boiling point. The solvent is a single phase during absorption but during the regeneration the solution forms two liquid phases when heated and stirred. The main advantage is the lower regeneration temperature of 80 °C that can be achieved without using steam. The cyclic loading capacity is high with 0.9 moles of CO_2 per mole of absorbent. Degradation of the solvent is minor, but volatility and thus losses of the solvent are a major problem. (Zhang et al. 2011a, b., Zhang et al. 2010.)

DMC+DPA

Zhang et al. (2010) have studied the mixture of N,N-dimethylcyclohexylamine (DMCA) and dipropylamine (DPA). DMCA acts as the main absorbent, because of its high CO_2 loading capacity in absorption and low residual loading upon regeneration, and DPA can be considered to act as an activator, due to its rapid CO_2 absorption kinetics. The blend in aqueous solution combines the advantages of both. However, the slow absorption rate of DMCA and the precipitation of protonated DPA ions and bicarbonates establish a real problem for its use as a solvent. (Zhang et al. 2010., Zhang et al. 2011a, b.)

B0+A1

The solvent B0 is a tertiary amine and thus it has a slow CO_2 absorption rate (72 g/l/h up to a CO_2 loading of 0.4 mol/mol). To accelerate the reaction, it is blended with an activator A1 with high absorption rate (130 g/l/h) that makes the reaction more than 80% faster than without an activator in the initial 30 minutes. (Zhang et al. 2010.)

In the regeneration step CO_2 is first liberated from the main absorbent B0. This forms a separate organic phase over the solution because of the limited aqueous solubility of B0. Also A1 dissolves in the organic phase as similar polarity of the amine molecules makes the organic phase to prefer it rather than the aqueous phase. B0 acts as an extractive solvent during regeneration, withdrawing the activator from the aqueous phase. It is important when enhancing the solvent regeneration rate. (Zhang et al. 2010.)

The cyclic capacity of the B0 and A1 blend is better than the previous blend DMCA+DPA. The most remarkable phenomenon is its rapid reaction rate in both absorption and desorption, since A1 not only serves as a solubiliser for B0 but also leads to a vigorous reaction with CO_2 right from the outset. However, the solvent losses due to vaporisation are even greater than for MEA. Also foaming is a disadvantage of this solvent. (Zhang et al. 2010.)

Activated dimethylcyclohexylamine

The solvent system of activated dimethylcyclohexylamine (a-DMCA) has dimethylcyclohexylamine (DMCA) as a regeneration promoter and alkanylamine A1 as an activator. (Zhang et al. 2011a, b.)

a-DMCA alone has around 50% higher net loading capacity than conventional MEA+MDEA. The absorption rate is relatively fast even at rich loading of 2.5 mol/l. This is due to its reaction by carbamate formation, carbamate conversion and bicarbonate formation. A1 has a good contact with both CO_2 and water in gas-liquid interphase, in the organic phase, at the liquid-liquid interface and in the aqueous phase during absorption. (Zhang et al. 2011a, b.)

Solvent also has good regenerability. After the CO_2 release in the stripper, a biphasic system establishes with water and organic phases intensifying the depth of regeneration. When the solution is cooled it automatically transforms back into a homogenous liquid phase. (Zhang et al. 2011a, b.)

The drawbacks of the solvent are the higher rate of foaming when compared with MEA and also significant solvent losses through vaporisation. Degradation is, however, less than with MEA mass fraction of 30%. (Zhang et al. 2011a, b.)

3.2 Liquid-solid solvents

3.2.1 Chilled ammonia for CO_2 capture

Compared to ammonia absorption at ambient temperature, the process of chilled ammonia has an advantage of lower ammonia slip in the absorber, decreasing flue gas volume and it also allows precipitation of several ammonium carbonate compounds in the absorber. In the method for chilled ammonia for CO_2 capture, a solid phase that consists of ammonia carbonate and bicarbonate is formed in the absorber. When it comes to finding solutions to decrease the energy requirements, the chilled ammonia process shows good results as it can absorb CO_2 at as low temperature as 2-10 °C and can reach stripper energy consumption of only 2 GJ/ton CO_2. In addition the process has high carbon dioxide capacity and is missing amine’s problems with degradation. (Darde et al. 2009.)

3.2.2 Deep eutectic solvents

Deep eutectic solvents (DES) are studied for substitutes of conventional ionic liquids used for CO_2 capture. DESs are ionic mixtures of solid compounds that form liquids at room temperature when mixed. DESs can form eutectics, which is a single chemical composition that solidifies at a lower temperature than any other composition of the same mixture or the individual compounds. Many of the solvents under study show glass transition points instead of (eutectic) melting points, which is why alternatively the name low transition temperature mixtures (LTTMs) is often used instead of DES. The mixtures contain usually a natural organic salt as the hydrogen bond acceptor and a natural organic acid as the hydrogen bond donor. DES has low volatility like ionic liquids, but in contrary to those it is non-flammable, less toxic, much cheaper, and often biocompatible and biodegradable. As they can be easily prepared from readily available starting materials the costs are competitive. (Zubeir et al. 2013., Francisco et al. 2013.)

Lactic acid + choline chloride

Francisco et al. (2013) showed that lactic acid + choline chloride mixture forms stable liquid in a wide range of compositions and also unusually low transition temperature. Despite its promising properties, it was found to have low CO_2 solubility. However, the formability of LTTM solvents opens rooms for further investigations in gas separation processes.

Nature based DES

In the study of Kroon (2013) plant cells forming DESs are studied. Plant protects its cells from severe conditions of high or low temperatures or drought by forming deep eutectic solvents from constituents in the cells. The potential for using this in CO_2 capture is under study.

3.2.3 Aminosilicones

Aminosilicones are one type of compounds that can be used as solvents in phase-change systems for CO_2 capture. They have properties such as low vapour pressure, high boiling point, thermal stability and low heat capacity. When compared with 30% MEA process, there are significant energy savings when non-volatile cosolvents are used. While the products of some aminosilicones with CO_2 are viscous liquids, waxes and sticky solids, in the studies of Perry et al. (2012) formation of carbamate salts were noticed when liquid aminosilicones were exposed to CO_2. These salts could be thermally decomposed to obtain pure CO_2 and to regenerate the aminosilicone. (Perry et al. 2012.)

The process starts with the formation of solid particles from a low viscosity liquid. The particles are formed when the liquid sorbent is sprayed into a CO_2-rich exhaust gas stream as a fine mist. As the droplet diameter is small and thus the surface are of it is large the mass transfer improves and promotes the rapid reaction with CO_2 to form carbamate salt particles. The sorbent remains effective also in the presence of moisture and the generated dry solids do not depend on the issue whether the CO_2 is dry or wet. The solid could be transported either as a dry powder flow or as a slurry with a lean liquid sorbent at high solid loading. (Perry et al. 2012.)

GAP-0

One example is the 1,3-bis(3-aminopropyl)-1,1,3,3-tetramethyldsiloxane, also known as GAP-0. When compared with non-phase-change aminosilicones, these show very good thermal stability, low vapour pressure and a high CO_2 loading capacity. The heat of reaction for the GAP- 0 has been reported to be 2 500 – 2 600 kJ/kg CO_2 absorbed, compared to 1 900 kJ/kg CO_2 for MEA. Also the absorption capacity compared to a 30% mass fraction of MEA system has been reported to be more than double as high. The GAP-0 process takes place at 2-5 bar pressure and the regeneration temperature is around 120 – 180 °C. (Perry et al. 2012.)

Patent of amino-siloxane sorbent

In capturing the CO_2 gas from the gas stream, the method for capturing CO_2 invented by Ayala & Perry (2013) utilizes a liquid phase-changing sorbent aminosiloxane compound that forms a solid in the presence of CO_2. The delivery developed facilitates the storage and generation of the purified CO_2 gas and liquid phase-changing sorbent. The solid reaction product is in the form of dry solid, wet solid, slurry, or fine suspension. The method is for gas flow comprising CO_2 that is called the pre-combustion synthetic gas or “syngas”. The CO_2 capture of the solvent takes place with a chemical reaction, and optionally physisorption. A new solid molecule is formed. The sorbent also relies upon a temperature swing process to facilitate the sorption and desorption of CO_2.

4 CARBON DIOXIDE CAPTURE WITH AQUEOUS DEEA+MAPA SOLVENT

Although formation of two liquid phases has its advantages it also makes the process more complicated. Liebenthal et al. (2013) propose only minor changes for the traditional process plant design of CO_2 capture with amines. A flow sheet for an aqueous DEEA + MAPA system can be seen in Figure 3.

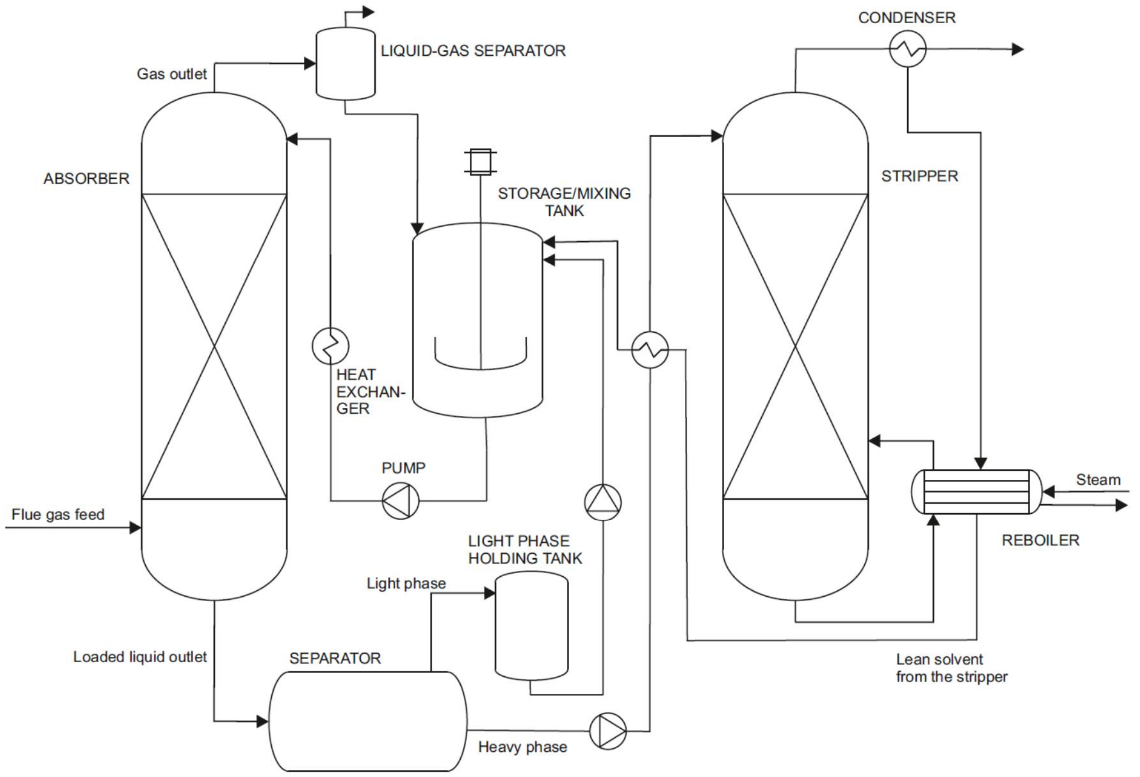

Figure 3. Flow sheet for carbon capture unit with phase change solvents (Liebenthal et al. 2013., Pinto 2014).

The process differs mainly from the MEA process by having an additional operation unit of separation. The CO_2 rich stream leaving the bottom of the absorber is taken to a separator. The loading with CO_2 has formed two liquid phases. In the separator the CO_2 rich and CO_2 lean phases are separated. Only the heavy phase rich with CO_2 is taken to stripper to be regenerated. It can be first heated by a heat exchanger with the stream returning from the stripper. After regeneration the solution is mixed with the light phase from the separator and fed back to the top of the absorber. The modifications for the DEEA + MAPA process lead to a lower liquid flow rate in the stripper.

4.1 Formation of two liquid phases

Compositions of the two liquid phases depend on various parameters like amine concentration in the solvent, CO_2 loading or solvent temperature. High amine solubility and a high dielectric constant are two important features that prevent liquid-liquid phase separation or precipitation, when a high amount of salt is produced by reaction of the amine and the acid gas. On the other hand the liquid-liquid phase can be intentionally formed and its properties exploited. (Raynal et al. 2011.) Two liquid phases can be formed in equivalent when the components of the mixture differ significantly and the values of activity coefficients are big. Amines can be classified in three categories based on liquid-liquid phase formation (Aleixo et al. 2011):

1. Amines that are fully soluble in water and do not exhibit liquid-liquid phase separation in conditions of the absorption process,
2. Amines that are not soluble in water at room temperature,
3. Amines that are soluble in water at room temperature, and exhibit a liquid-liquid phase separation in a given amine concentration range, either by an increase in the loading or by an increase in temperature.

Most of the amines commercially available belong to the first category that cannot be used as phase change solvents. Neither can the second category as the two phases would exist also in the absorber, where contact between the flue gas and the solvent is critical. Use of these might lead to absorber oversizing, especially tertiary amines that need to be in contact with water in order to react with carbon dioxide. (Aleixo et al. 2011.)

Some amines display a Lower Critical Solubility Temperature (LCST). The two-phase region obtained at high temperatures is the combination of physical phenomena, phase separation due to an increase in the loading and phase separation due to an increase in temperature. The solvent should have liquid-liquid phase separation at low amine concentration and a low loading. (Aleixo et al. 2011.)

During the experiment of Pinto et al. (2011) at a certain point of loading the clear mixture became cloudy and droplets could be seen on the walls of the absorber. It was indicating the two-phase region, which was formed by the end of the experiment. The mechanism of forming two liquid phases is explained by Xu et al. (2013) by a limited solubility of the solvent acting as activator into the reaction products of CO_2 with the solvent with a faster reaction rate. At lower loadings the amount of activator increases in the upper phase and the amount of solvent with faster reaction rate increases in the lower phase. However, at higher loadings the amount of activator decreases in the upper phase and increases in the lower one while the amount of the other solvent stays almost constant. CO_2 has first reacted with the solvent with a faster reaction rate and due to limited solubility of the activator into the reaction products and due to its relatively smaller density, some of it is separated and transfers to the upper phase. The activator now starts to react with CO_2 while the other solvent has already reached equilibrium. As the reaction products of the activator and CO_2 are soluble with the reaction products of the other solvent they now transfer to the lower phase and mix till the equilibrium is reached.

Also Ciftja et al. (2013c) observes that while the partial pressure of the CO_2 is increased the DEEA/MAPA ratio in the lower phase increases and for the upper phase decreases. It is assumed the upper phase rich with DEEA further absorbs CO_2 and then dissolves into the lower phase. In fact, above a certain CO_2 loading (above $\alpha = 0.23$ for 1 M MAPA + 5 M DEEA), the two liquid phases become again one. At higher temperatures the DEEA absorption capacity is lower and thus the two phases remain. Finding the critical CO_2 loading with two liquid phases is thus important to have reasonably high loading with low heat of absorption without losing the benefit of two phases. (Arshad et al. 2013b.) In the study of Arshad et al. (2014) it is noted that at 40 °C and amine concentration of 5 M DEEA + 2 M MAPA the isotherm of CO_2 partial pressure against loading is quite steep up to the CO_2 loading of around 0.45 mol CO_2/mol amine. The behaviour is similar to that of the H_2O-MAPA-CO_2 system. After this the slope of the line decreases in a similar way as that of the H_2O-DEEA-CO_2 system. It can be assumed that at certain loading after this point the two phases become again one.

Also Uusi-Kyyny (2014) observed formation of two liquid phases with the increasing CO_2 loading (see Figure 4). Also remarkable warming up of the separation funnel when CO_2 was fed is reported. The lower phase was cooler than the upper phase, which indicates that the reaction takes place in the upper phase (Uusi-Kyyny 2014). It is because the warming is due to exothermic reaction. The product that is no longer soluble with the solvent of the upper phase then settles to the lower phase.

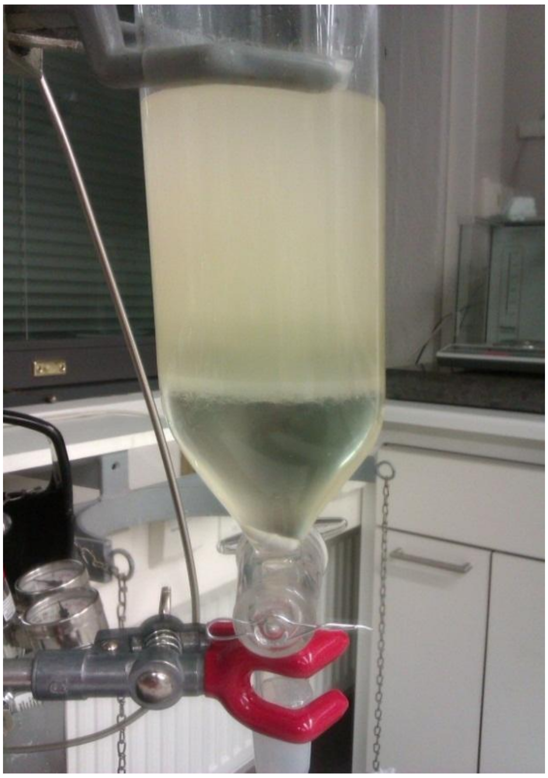

Figure 4. Settling of two liquid phases after CO_2 bubbling (Uusi-Kyyny 2014).

4.2 Separation of two liquid phases

Traditionally, a gravity decanter or other separator is chosen and designed based on the size of dispersed drops. However, this information is rarely available for a new process. Also the rate of the drop coalescence is needed. Whether the system is fast-coalescing or slow coalescing can be determined by making a simple shake test for the feed material. (Frank et al. 2008.) The literature survey shows that the settling time of a loaded aqueous DEEA + MAPA system is relatively long. In the study of Arshad et al. (2013b) of amine solution DEEA + MAPA + H_2O the system took time from 60 to 90 minutes to reach equilibrium or in some cases even more. Pinto et al. (2013) left the pilot of the loaded system to stabilize for 6 hours after changes. To speed up the separation between the phases a centrifuge can be used (Pinto 2014). The separation times for the two liquid phases depending on temperature are 25-30 minutes in 40 °C, 9-12 minutes in 60 °C and only 3-5 minutes in 80 °C (iCap 2013). However, the factors affecting the separation time like loading of carbon dioxide in the solvent or concentration of amine are not given.

In general intermolecular forces cause liquids surface tension and the same way the interactions on a liquid-liquid boundary make interfacial tension. If liquid A is in contact with liquid B, an interfacial tension exists between them. (Bailey 2010.) If the layers do not separate, the reason is often that the mixture has been shaken too vigorously, which forms an emulsion instead of two layers. To fasten the separation of the liquids, the mixture can be mixed slowly to bring the small droplets together, which results in the formation of a new layer. Centrifugation and gravity filtration can work also. In a batch process the bottom layer is removed first as it is easier to do. (Frank et al. 2008.)

4.3 Commercial availability of the solvents

Most of the amines commercially available are fully soluble in water and do not exhibit liquid-liquid phase separation in conditions of absorption process. They cannot be used as phase change solvents. (Aleixo et al. 2011.) The solvents DEEA and MAPA are both globally available and affordable (Bacher 2013).

4.4 Patents

Rojey et al. (2009) have published a patent for their discovery that some solvents with special structures can separate into two liquid phases after absorption and heating, but they did not give the particular structures.

Cadours et al. (2012) have patent for deacidizing a gaseous effluent that has at least one acid compound of the group including hydrogen sulphide (H_2S), mercaptans, carbon dioxide (CO_2), sulphur dioxide (SO_2), carbon polysulphide (COS) and carbon disulphide (CS_2). The absorbent solution is selected for its property to form two separable phases when it absorbs an amount of acid compounds. The two phases are separated and the phase with acid compounds is regenerated. Finally, both phases are recycled in the process.

In the study and patent of Hu (2009) it is stressed that biphasic solvents consist of several compounds, including at least one activator A and one solvent B, and that the mixture composition should be 20% A plus 80% B. Hu (2009) did not give the exact amines in the solvents.

5 REACTIONS FOR THE ABSORPTION OF CO_2 WITH DEEA + MAPA SYSTEM

The absorption of CO_2 in aqueous amine solutions is based on three mechanisms that are the zwitterion mechanism, the termolecular mechanism and the base catalysed hydration mechanism. Primary, secondary and sterically hindered amines are usually described by the zwitterion mechanism while reaction of tertiary amines with CO_2 follows the base catalysed hydration mechanism. (Majeed 2013.)

CO_2-water system and formation of bicarbonate

First a physical process of dissolution of the gaseous form of CO_2 occurs. In the dissolution of CO_2 into water a carbonic acid is formed. It deprotonates and forms bicarbonate HCO_3^-. It exists in equilibrium with carbonate and carbonic acid, but generally under absorber conditions bicarbonate predominates. The position is dictated by pH and it has an effect on CO_2 to amine ratio. In this step amine acts simply as a base.

Dissolution of CO_2 from the gas phase to the liquid phase:

$$CO_{2(g)} \leftrightarrow CO_{2(l)} \qquad (2)$$

Dissociation of water:

$$2H_2O \leftrightarrow H_3O^+ + OH^- \qquad (3)$$

Dissociation of dissolved CO_2 through carbonic acid:

$$2H_2O + CO_2 \leftrightarrow H_3O^+ + HCO_3^- \qquad (4)$$

Dissociation of bicarbonate:

$$HCO_3^- + H_2O \quad \leftrightarrow \quad H_3O^+ + CO_2^{2-} \qquad (5)$$

The absorption for generic amine R_1R_2NH

Dissociation of protonated amine:

$$H_2O + R_1R_2NH_2^+ \quad \leftrightarrow \quad H_3O^+ + R_1R_2NH \qquad (6)$$

where R_1R_2NH is alkanolamine
$R_1R_2NH_2^+$ is protonated amine.

Carbamate reversion to bicarbonate (for primary amines) :

$$H_2O + R_1R_2NCOO^- \quad \leftrightarrow \quad R_1R_2NH + HCO_3^- \qquad (7)$$

where $R_1R_2NCOO^-$ is primary amine carbamate ion.

The absorption process in primary and secondary amines such as MAPA

Two molecules of amine are required to absorb one molecule of CO_2 in carbamate formation. The other one reacts with CO_2 to form carbamate and the other acts as a base and reacts with the released proton. Reversing this reaction requires a lot of energy.

Dissociation of protonated MAPA:

$$MAPAH^+ + H_2O \quad \leftrightarrow \quad MAPA + H_3O^+ \qquad (8)$$

where $MAPAH^+$ is protonated 3-(methylamino)propylamine

$$MAPAH^{2+} + H_2O \quad \leftrightarrow \quad MAPAH^{2} + H_3O^{+} \tag{9}$$

where MAPAH^{2+} is di-protonated 3-(methylamino)propylamine.

Formation of MAPA carbamates:

$$MAPA + CO_2 + H_2O \leftrightarrow MAPACOO_p^- + H_3O^+ \tag{10}$$

where MAPACOO$_p^-$ is 3-(methylamino)propylamine carbamate (primary)

$$MAPA + CO_2 + H_2O \leftrightarrow MAPACOO_s^- + H_3O^+ \tag{11}$$

where MAPACOO$_s^-$ is 3-(methylamino)propylamine carbamate (secondary).

Dissociation of protonated carbamates:

$$MAPACOO_P^- + H_2O \leftrightarrow MAPACOO_P^- + H_3O^+ \tag{12}$$

$$MAPACOO_s^- + H_2O \leftrightarrow MAPACOO_s^- + H_3O^+ \tag{13}$$

Di-carbamate formation:

$$MAPACOO_p^- + CO_2 + H_2O \leftrightarrow MAPA(CO_2^-)_2 + H_3O^+ \tag{14}$$

$$MAPACOO_s^- + CO_2 + H_2O \leftrightarrow MAPA(CO_2^-)_2 + H_3O^+ \tag{15}$$

where MAPA(CO$_2^-$)$_2$ is 3-(methylamino)propylamine dicarbamate

The base reactions in tertiary alkanolamines such as DEEA

Amine protonation:

$$\mathrm{DEEA} + H_3O^+ \leftrightarrow \mathrm{DEEAH}^+ + H_2O \qquad (16)$$

Base catalytic effect on hydration of CO_2:

$$\mathrm{DEEA} + CO_2 + H_2O \leftrightarrow \mathrm{DEEAH}^+ + HCO_3^- \qquad (17)$$

where DEEAH^+ is protonated 2-(diethylamino)ethanol.

(Ciftja et al. 2013c., Hessen et al. 2011., McCann et al. 2008., Majeed, 2013.)

5.1 The speciation and quantities of species in the system

It is important to characterize liquid-phase composition, as it is needed for both modelling of liquid vapour equilibrium and absorption kinetics in CO_2 absorption processes. Speciation must be mostly concluded. To calculate the concentrations of the species their activities are defined. The electrolyte NRTL and the extended UNIQUAC electrolyte models are commonly used to predict the activity coefficient and the mole fraction of the product. However, it is difficult to estimate the actual mole fraction. The uncertainty of the mole fraction also affects the mass transfer model and thereby the design and scale-up ability of a simulation model. Ciftja et al. (2013c) have used nuclear magnetic resonance (NMR) spectroscopy for accurate measurements of individual ionic species or species groups. It can be used to complete the other properties used for fitting the thermodynamic model, and for making the actual speciation. (Ciftja et al. 2013a.)

Potential species to be found in the loaded solution of DEEA and MAPA are DEEA, DEEAH^+, MAPA, MAPAH^+, $\mathrm{MAPACO_2}^-$ (p) (primary), $H^+\mathrm{MAPACO_2}^-$ (s) (secondary) and $\mathrm{MAPA(CO_2^-)_2}$ (dicarbamate). High pH in the solution makes the existence of di-protonated MAPA unlikely. The species H_2O, $H3O^+$, OH^-, CO_2, HCO_3^- and CO_3^{2-} are also present. Amine-protonated amine, amine carbamate -protonated amine carbamate and bicarbonate-carbonate involve proton transfers. They have very fast reaction rates and very short relaxation times. This is why 13C NMR gives the average of the peaks of these species. (Ciftja et al. 2013c.)

In the studies of Ciftja et al. (2013c) species formed in CO_2 loaded solutions of 5 M DEEA and 2 M MAPA are for the upper phase mainly DEEA. Also very low peaks of carbamate, and dicarbamate are found but no carbonate-bicarbonate. They are difficult to quantify because of their very low signal intensities. For the lower phase more of these peaks are better observed. The main products are identified to be primary carbamate, secondary carbamate, both including protonated forms, dicarbamate and bicarbonate-carbonate.

Speciation can also be made for different forms of absorbed CO_2, which include dissolved CO_2, carbonic acid, bicarbonate and carbonate. According to McCann et al. (2008) CO_2 is present predominantly as carbamate at all temperatures.

6 GAS SOLUBILITY

Vapour-liquid equilibrium or gas solubility is the relationship between the concentration of acid gas in the solution and its partial pressure in the gas phase at equilibrium. It is important data when designing a treating plant as it determines the liquid rate necessary for complete or economic solute recovery. (Kohl & Nielsen 1997.)

Typically the solubility of CO_2 in aqueous amine solution is described as CO_2 loading as a function of its partial pressure or more precisely, of its fugacity. According to Kohl & Nielsen (1997) the CO_2 loading is the absorption capacity of the solution that is defined as moles of CO_2 absorbed per mole of amine in solution

$$\alpha = \frac{n_{\mathrm{CO2}}}{n_{\mathrm{amine}}} \tag{18}$$

where α is the molar capacity
n_{CO2} is the molar amount of CO_2
n_{amine} is the molar amount of amine.

In the study of (Ciftja et al. 2013c) the loading is measured as a function of the partial pressure of CO_2 in the range from 1 to 20 kPa. It is noticed that the lower phase is mainly loaded with increasing DEEA to MAPA ratio as a function of the partial pressure. The study of Arshad et al. (2014) is about the effect of partial pressure and temperature on the loading. The loading increases with increasing partial pressure but decreases with a temperature rise. In the studies of Arshad et al. (2013b) and Kim & Svendsen (2011) the heats of absorption is found to increase with the CO_2 loading. The study also shows how forming of the two liquid phases depends on the loading. CO_2 loading is increasing the volume of the lower phase and makes it viscous. With the loading high enough it can again become one phase.

As solubility varies not only with the partial pressure of the acid gas but also with the change in temperature, type of amine, amine concentration in the solution and nature and concentration of other components in the solution, the amount of data required to consider all different conditions is enormous. Correlations have been developed to predict VLE relationships when the specific data is not available. For the preliminary studies experimental data is useful but correlations are needed for interpolating and extrapolating data to specific conditions and designing the system with computer programs. (Kohl & Nielsen 1997.)

6.1 DEEA + MAPA concentration

According to the study of Majeed (2005) 2 M MAPA + 5 M DEEA (2M5D) is the best concentration giving the lowest Henry’s constant. The smaller the Henry’s constant the better is the physical solubility. In the study of Arshad (2014) the concentrations 2M5D and 1M5D both gave better results than the reference MEA. The ratio 2M5D is used in several studies (Ciftja et al. 2013c., Arshad et al. 2013b., Liebenthal et al. 2013., Pinto et al. 2014). However, in the study of Majeed (2005) the points 3M1D, 3M3D and 4M3D were not tested but the solubilities in these three cases are obtained by interpolation from experimental data points. Also the increase in DEEA is not tested further than for 5 M, but as water is necessary for the reaction between CO_2 and DEEA the concentrations cannot be too high. Also high concentrations can cause problems like volatility or precipitation. It is preferable for amine to be needed in only small amounts for CO_2 absorption.

7 ENERGY BENEFITS

Energy consumption is one of the main problems of traditional CO_2 capture methods with amine. The heat duty needed for solvent regeneration in the reboiler of the capture plant is often the largest contributor to the energy efficiency of the overall process. However, the lowest heat duty does not generally lead to the lowest overall energy consumption. The other quantities affecting the efficiency are electrical duty of the CO_2 compressor, pumps and blowers and circulation pumps for the large amounts of cooling water needed in the capture and compression processes. (Liebenthal et al. 2011b., Liebenthal et al. 2013.)

As the novel phase change system forms two liquid phases after absorption, it can be utilized to reduce energy consumption. Carbon dioxide concentrates in the other phase and it can be separated based on difference in density. This means that only a part of the solution must be taken to the stripper for regeneration, which reduces the need for thermal energy remarkably. (Liebenthal et al. 2013.)

Liebenthal et al. (2013) have simulated the process with CO2SIM and give the liquid to gas (L/G) ratio as a function of the reboiler heat duty to have the 90% CO_2 capture rate. The lowest heat duty is achieved at lower pressures with a low L/G ratio. However, decreasing the L/G ratio means an increase in the reboiler temperature. This again leads to higher steam pressures. Thus the optimal overall efficiency operation point differs from the operation point of the lowest heat duty, as the reboiler temperature overcompensates the benefits of the lowest heat duty. Also the benefits of the elevated desorber pressure to reduce the energy consumption of CO_2 compression need to be considered as compensation of heat duty.

The study also shows that the energy consumption and the net efficiency penalty are remarkably lower for the solvent DEEA + MAPA than for MEA even with higher solvent flow. It is estimated that the potential for reducing capture plant’s thermal and recompression energy requirements is even 45-50% for the studied Greenfield post-combustion plants and retrofits. It also reduces significantly the plant size and thus capital costs. (Liebenthal et al. 2013.)

The reboiler duties are compared in Appendix 1, Table 14, where the DEEA + MAPA blend seems to have lowest reboiler duties. The comparison is however only an approximate as conditions differ and CO_2 capture percentage and the achieved lean amine CO_2 loading that are important for the evaluation are unknown for some of the cases. The low CO_2 loading in the lean amine flow enables the recycling of the solution, which seems good for DEEA + MAPA. In Table 1 an example of efficiency penalties of the CO_2 capture plant are presented. It shows that heat duties have the highest efficiency penalties.

Table 1. Efficiency penalties of CO_2 capture systems under study in iCap (Liebenthal 2011a).

Efficiency penalties in %, Liebenthal et al. (2011a)	MEA	Liquid-liquid
Heat duty	6.26	3.36
Cooling duty	0.19	0.24
Auxiliary power duty	0.44	0.92
Compressor duty	2.87	2.23
Drying heat duty	-	-
Flue gas desulfurization unit	-	-
Heat integration (from flue gas to preheating train)	-	-
Overall	9.79	6.75

7.1 Heat of absorption

Heat of absorption is an important property as it is directly related to the energy used for the regeneration of the solvent. The difference between enthalpy of absorption and desorption in heat of absorption is around 25-30% (Arshad et al. 2013b). According to the study of McCann et al. (2009) the difference between absorption and desorption enthalpy comes significant at higher partial pressures.

The value of the heat of absorption is mainly dependent on the amine group functionality, thus it is higher for primary amines and the lowest for tertiary amines. (Kim & Svendsen 2011.) Heat of absorption depends on temperature and the type of amine used. Tertiary amine DEEA seems to be more dependent on these parameters compared to MAPA. In mixtures heats of absorption depend on CO_2 loading, temperature and composition of constituent amines in the mixture. (Arshad et al.

2013b., Kim & Svendsen 2011.) Pressure and amine concentration do not significantly affect the heat of absorption within the range studied (Kim & Svendsen 2011). However, according to the study of Arshad et al. (2013b) the heat of absorption is independent of the partial pressure of CO_2 above the solution, when the solvent concentration is fixed. Also there is no effect when CO_2 feed pressure is fixed but solvent concentration changed at least if the change is minor.

7.2 Vapour pressures of pure compounds of the solution

Data on the total vapour pressure of amine solutions as a function of temperature and amine concentration is necessary for the design of stripping columns and reboilers (Kohl & Nielsen 1997). Hartono et al. (2013) have measured the vapour pressures of DEEA and MAPA. It is seen that MAPA is more volatile than DEEA as it does not have an alcohol group in its molecular structure. The data from the literature for DEEA cover wide temperature range of 5-203 ˚C while for MAPA it is only 54-139 ˚C. Hartono et al. (2013) have however made an extrapolation of the data with a good accuracy. The data has been used to determine parameters for the Antoine equation.

8 PHYSICAL PROPERTIES

The most important physical properties influencing the transport are the liquid-liquid interfacial tension, liquid density and viscosity. The diffusion of CO_2, formation and coalescence of drops are affecting the liquid-liquid contactors and phase separators. (Frank et al. 2008.)

8.1 Density

Density of the liquid is important as it can be used to separate two immiscible phases. The higher the density difference is the better and quicker can the separation be made. Density changes due to the solubility of the chemical that dissolves in water and the organic solvent. This can be used as an advantage. Solubility and density differences have been studied by Arshad et al. (2013b) for a loaded DEEA + MAPA mixture for which the increase in solubility increases the density of the lower phase.

Majeed (2013) studied the densities of both MAPA and the mixture of DEEA + MAPA. In both cases the increase in temperature decreases the density of the system. When the concentration of the amine is increased the density is rather related to the overall total molar concentration than the individual amine constituent. The increase in the concentration of DEEA with constant MAPA decreases the density of the blended system. (Majeed 2013.)

8.2 Viscosity

Viscosity of both liquid and gas phases are affected by temperature changes but usually pressure affects only the viscosity of the gas phase. The viscosities of aqueous amine solutions are affected by the components dissolved into it. The study of Arshad (2013b) shows that the CO_2 loaded aqueous DEEA + MAPA mixture is relatively more viscous than the unloaded feed solution. After the phase split the lower phase rich in CO_2 was more viscous than the upper phase lean in CO_2. Arshad (2013) speculates the increase in viscosity during CO_2 absorption may have a negative effect on the CO_2 absorption capacity.

In the study of Majeed (2013) for MAPA and aqueous DEEA + MAPA viscosities it is observed that with increasing temperature the viscosity decreases. With the decrease in temperature the viscosity values for different concentrations begin to differ increasingly. The viscosity increases exponentially with the increase in the DEEA concentration. In general the increase in the concentration of amine in the blended system causes vast changes in viscosities especially at low temperatures. Although an increase in the temperature can lower viscosity it might not be beneficial for temperature-sensitive materials. The viscosity can also be decreased with solvents by dilution, but accuracy is needed. (Majeed 2013.)

8.3 Density and viscosity of loaded solvent

Uusi-Kyyny (2014) has performed density and viscosity experiments for 5 M DEEA + 2M MAPA solvent mixture. The solvent was loaded with CO_2 and the formation of two phases visually followed. Finally the densities and viscosities of the two liquid phases were measured after two hours of CO_2 feed.

The amount of absorbed CO_2 affects viscosity and density. It can be calculated from the difference between the total mass before and after the CO_2 feed. The results for the CO_2 loading from the experiments of Uusi-Kyyny (2014) are presented in Table 2. Water evaporation is not considered. The loading from his experiment is found relatively low when compared with the results Arshad et al. (2013d) has achieved.

Table 2. The increase in the mass of the solution after CO_2 feed[a], CO_2 molar mass[b], molar amount[c] and its loading[d].

After loading	m^a [g]	M^b [g/mol]	n^c [mol]	α^d [mol_{CO2} / mol_{amine}]
CO_2 (Uusi-Kyyny 2014)	15.1	44.01	0.343	0.196

The densities and viscosities from the experiment of Uusi-Kyyny (2014) for the two liquid phases formed after loading are compared with values for unloaded solvent (see Table 3). The solvent concentrations are 5 M of DEEA and 2 M of MAPA. This data is used later in this thesis to calculate the size of a gravity settler.

From the Table 3 it can be observed that the density of the lower heavy phase is remarkably higher due to the CO_2 loading. The density of the light phase is almost the same as the density of the solvent blend before the CO_2 loading.

Uusi-Kyyny (2014) reported that the viscosity of the heavy phase decreased during the measuring, which indicates the CO_2 escape due to an open cup used in the equipment. The highest value was measured at the beginning of the measurement. The heavy phase was very viscous and syrup-like (Uusi-Kyyny 2014). The viscosity of the upper phase is lower than the viscosity given by Majeed (2013) for the unloaded solvent blend. It is close to the value of 5 M DEEA, which indicates that it consists mainly of DEEA like stated in previous studies of Ciftja et al. (2013a) and Arshad (2013a).

Table 3. The densities and viscosities for the light and heavy phases and for an unloaded solvent at around 20 ˚C.

T=20 ˚C	Density [g/cm^3]	Viscosity [cP]
Light phase (Uusi-Kyyny 2014)	0.92817	12.6
Heavy phase (Uusi-Kyyny 2014)	1.11438	550-1480
Unloaded (one phase) (Majeed 2013)	0.92572	19.4
DEEA 5 M (*T*=25 ˚C) (Xu et al. 2013b)	0.96	12
MAPA 2 M (*T*= 20 ˚C) (Majeed 2013)	0.98905	2.7

8.4 Physical CO_2 solubility

CO_2 can be chemically bound to an absorbent but in physical solubility it is in the form of free CO_2 in absorbent solution. According to the Henry’s law the amount of physically absorbed gas increases with the increase in its partial pressure. Physical absorption is more noticeable if partial pressure of the absorbed gas is high. It also depends upon the temperature as at low temperatures the absorption is more efficient. (Majeed 2013.)

The knowledge of the physical solubility of CO_2 at numerous concentrations and temperatures is needed to develope a kinetic model for the system. However, the direct measurement of physical solubility is not possible because CO_2 reacts with amine. Majeed (2013) has used N_2O, which is a non-reacting gas, with amine solutions to measure the physical solubility.

According to experimental results of Majeed (2013) temperature of the amine solution and the amine molar concentration has a significant effect on the absorption rate. With the increase in molar concentration and temperature the rate of absorption increases. Another important factor is the mass transfer area that has an influence on the flux. When mass transfer area is decreased the flux of CO_2 or the absorption rate increases.

8.5 Freezing point depression

The interaction between CO_2 and the solvents can be deduced from the measured freezing points in the CO_2 loaded systems. Arshad (2013d) has measured the freezing points for binary aqueous DEEA and MAPA solutions and a ternary aqueous DEEA + MAPA solution with different loadings. The water-MAPA freezing point values showed the highest deviation from ideal situation to that of MEA, MDEA and DEEA, which indicates that the MAPA-water interaction is higher than the others have. The data can be used for thermodynamic modelling of CO_2 absorption-desorption systems. Water activity data can be very accurately determined from the measured freezing point data.

9 DEGRADATION AND IMPURITIES

As impurities change the thermodynamic properties of the CO_2 stream they may cause undesired effects during the process, transportation or in the destination. Volatile products can leave with flue gas to the environment and nonvolatile make up the reclaimer waste. (Rochelle et al. 2011.) Amines will start degrading to other products, which must be taken into consideration and minimized. Specific information of the effects on the DEEA and MAPA system is not always found, thus some of the problems are discussed in this work over the amine system instead.

9.1 Gas stream compositions

9.1.1 Flue gas

Flue gas is generally the combustion gas of a power plant. Its composition depends on what is burned. The requirements for the purity of flue gas are dependent on the purpose of use and the transportation. Different impurities to be considered when handling the flue gas are as follows (U.S. Environmental protection agency 2013a., Mikunda 2012., Suvanto 2013):

- Particles such as fly ash or soot are usually removed in a cyclone or electrostatic precipitator before the CO_2 capture to avoid their influence. Particles emissions can also be formed in the CO_2 capture when using solid sorbents or even with liquids,
- Mono-nitrogen oxides NO_x are usually removed from flue gas with the selective catalytic reduction process,
- For sulphur oxides SO_x the removal is often done with the flue gas desulfurization methods,
- Dehydration of the CO_2 stream or other means like hydrate inhibitors are used to prevent water from condensing as it might cause corrosion, pressure drops or even plugs,

- Non-condensable gases such as nitrogen, argon, excess oxygen and NO_x can be removed by flashing after capture and compression of CO_2, when the stream is in a liquid state.

9.1.2 Synthesis gas

Synthesis gas or syngas is a combination of hydrogen, carbon monoxide, and carbon dioxide. Synthesis gas is produced when carbon monoxide and water react and form carbon dioxide and hydrogen. Technology called integrated coal gasification combined cycle (IGCC) is used for the production. It can gasify coal, liquid hydrocarbons, natural gas, refinery wastes, biomass or other materials. In these plants pre-combustion capture is a considerable option to remove CO_2 during the process. The capture itself is very affordable and the combustion technology is considered to have reduced emissions compared to other power systems. (Ayala & Perry 2013.)

9.1.3 Hydrotreater refinery gases

According to U.S. Environmental Protection Agency (2013b) natural gas is sour when it contains H_2S more than 5.7 milligrams per normal cubic meters (mg/Nm^3). Sour gas is treated at processing facilities called desulfurization plants. H_2S is mostly removed by absorption in an amine solution, whereas other methods are carbonate processes, solid bed absorbents and physical absorption.

The hydrodesulphurization (HDS) unit in the petroleum refining industry is also often referred to as a hydrotreater. The hydrodesulphurization of petroleum fractions has long been a part of refining operations. It is the only method that can generally be applied for all kinds of sulphur compounds. Hydrogen reacts with organic sulphur compounds in the presence of a catalyst in the feedstock to produce hydrogen sulphide. The hydrogen rich gas is then separated from the liquid (or gaseous) hydrocarbon products. (Speight 1999: 10.)

An amine contactor is used to remove H_2S from the hydrogen rich gas and hydrogen can then be recycled. The amine gas treating is also used for the separated liquid with hydrocarbons. The liquid is first taken to the stripper. The overhead sour gas from the stripper contains hydrogen, methane, ethane, hydrogen sulphide, propane, and maybe some butane and heavier components. It is sent to the refinery's central gas processing plant for the removal of hydrogen sulphide in the refinery's main amine gas treating unit. If the feed contains olefins (for example, the feed is a naphtha derived from a refinery fluid catalytic cracker (FCC) unit), then the overhead gas from the HDS stripper may also contain some ethene, propene, butenes and pentenes, or heavier components. (Gary & Handwerk 2001.)

9.2 Degradation of alkanolamines

Alkanolamines are susceptible to both thermal and oxidative degradation. Thermal degradation limits the maximum temperature that can be allowed for the stripper. Tertiary amines degrade by arm switching and elimination at 120-140 ˚C. Diamines degrade by polymerization and urea formation at 100-130 ˚C. (Rochelle et al. 2011.) MAPA has high biodegradability and when it comes to thermal degradation it is relatively stable without CO_2. However, in the presence of CO_2 MAPA has high degradation. The thermal degradation begins with the formation of tetrahydro-1-methyl-pyrimidinone from reaction of MAPA with CO_2. Reaction of tetrahydro-1-methylpyrimidinone with MAPA can result in a variety of products, including urea, N-substituted pyrimidinones, and MAPA dimmer. The optimal combination would be stability under process conditions and at the same time being sufficiently biodegradable. (Eide-Haugmo et al. 2011.)

The oxidative degradation is most likely to take place in the absorber or after the emission release. For more resistant amines oxidation takes place in the heat exchanger instead of the absorber. (Rochelle et al. 2011.) According to Thomsen (2013) they react and degrade in contact with oxygen, CO_2 and SO_2 having degradation products such as

- oxaxolidinones and imidazolidinones,
- piperazine and carboxylic acids,
- amides,
- amines and nitrosamines, that are carcinogens,
- aldehydes,

- heat stable salts.

Nitrosamines are probably the most harmful degradation products as they can cause cancer, contaminate drinking water and impair aquatic organisms.

9.2.1 Sulphur dioxide

The SO_2 concentration in the flue gas is typically 0.0003-0.0005. The amine capture requires often high concentrations of it in the flue gas to make solvent consumption and make up costs in reasonable values. The optimal SO_2 content before the CO_2 removal is often a cost trade-off between CO_2 solvent consumption and SO_2 removal costs. (IPCC 2005.)

A high concentration of SO_2 in a simulated flue gas stream increases hydrogen ion concentration generated by SO_2 and H_2O as well as SO_2, O_2, and H_2O causing corrosion. Iron may also react directly with SO_2 and O_2 to cause corrosion of carbon steel. Corrosion caused by SO_2 forms products such as $FeSO_4$ and $2Fe_2O_3 * H_2O$. However, the CO_2 loading has the strongest impact on the corrosion rate, while SO_2 and O_2 show only slight effects. (Kladkaew et al. 2011.)

When the gas contains both H_2S and CO_2 they have an effect on the vapour pressure of each other. Amine holds carbon dioxide more tightly than H_2S as it is a stronger acid in solution. This is why H_2S/ CO_2 ratio in the equilibrium vapour over the rich solution is usually higher than in the gas feed. (Kohl & Nielsen 1997.)

iCap (2011) has studied a process where both SO_2 and CO_2 are removed in one gas/liquid contacting step. Currently available SO_2 scrubbing spray towers can be modified to capture both SO_2 and CO_2. By using the step-wise regeneration, two different streams are achieved, one gypsum stream and one CO_2 stream. This CO_2 stream should contain no detectable SO_2. The aim is to intensify the process, reduce capital costs and decrease energy requirements.

9.2.2 Oxygen

Usually flue gas contains 3-8% of oxygen. Lepaumier et al. (2009b) studied oxidative degradation mechanisms for amines at 140 °C under air pressure (2 MPa) in stainless steel reactors for 15 days. Most studied amines have degradation effects like demethylation, methylation (except for amines with no methyl group), dealkylation reactions and in a smaller amount, carboxylic acids formation. Volatile compounds (ammonia, methylamine, dimethylamine, trimethylamine) are also formed. Each amine family has also some special reactions: few ethanolamines oxidize into amino-acids; ethylenediamines always give piperazinones. This means that the replacement of the alcohol function by one second amine function does not affect significantly the overall oxidative degradation. The degradation rates and carboxylic acids amounts are very close, but, on the other hand, the main degradation compounds are not the same. (Lepaumier et al. 2009b.)

Tertiary amines are more stable than primary amines and secondary amines (Lepaumier et al. 2009b). In fact, tertiary amines seem to be oxidation inhibitors in blends with other amines. Auto-oxidation is inhibited probably by scavenging peroxides, but under high oxygen pressures (up to 150 bar) and temperature of 100 ˚C in polar solvents tertiary amine N-oxides can be formed. These products are not known to be carcinogenic, dermal sensitizers or cause reproductive toxicity. (Katritzky et al. 1995.) Steric hindrance also decreases degradation, as highly volatile compounds are not formed. In opposite to the degradation study with CO_2 the cyclic structure does not permit a better chemical resistance than its homologous linear molecule. (Lepaumier et al. 2009b.)

The increase in oxygen concentration increases also the corrosion rate. The higher the oxygen concentrations is the higher the dissolved oxygen present in the tested solution is resulting in the dissolution of iron. (Kladkaew et al. 2011.)

MAPA

According to the study of Voice (2013) MAPA degrades rapidly in the presence of oxygen, which makes problems for CO_2 capture from flue gas where oxygen is always present. Ammonia is produced when MAPA is contacted with oxygen and as a volatile product it can leave with the flue gas. Ammonia is classified to be dangerous for the environment. The ammonia production is reduced by an inhibitor A, which suggests the oxidation can potentially be inhibited. Also an addition of metal salts decreased the degradation of MAPA while it increased for the reference MEA.

9.2.3 Carbon dioxide

Lepaumier et al. (2009a) noticed that the use of high CO_2 pressure increases the amine degradation rate. CO_2 partial pressure and temperature are the highest in the stripper, which might cause amine degradation due the presence of CO_2. The secondary amines are the least stable. Also if a molecule has or can give the $-NH-CH_2-CH_2-NH-$ structure imidazolidinones are formed that decrease the absorption efficiency. Oligomers and cyclic compounds are formed when a compound has both a good leaving group and a nucleophilic function. However, some structures are stable in the presence of CO_2 like cyclic, hindered primary, and tertiary amines. (Lepaumier et al. 2009a.) MAPA showed thermal degradation of 50% in mass fraction in the presence of CO_2, while it is stable without it (Eide-Haugmo et al. 2011).

9.2.4 Mono-nitrogen oxides

Degradation product predictions of Mitch (2013) for several amines is based on earlier studies (Lepaumier et al. 2009a, b) and predicted nitrosamine and nitramine byproducts were based upon the structures of the solvent amine and its expected decay products when exposed to carbon dioxide, oxygen and NO_x. It is probable that in the absorber conditions NO_2 is mostly absorbed by reaction with secondary and tertiary amines that produce nitrite. However, in the stripper where temperatures can be from 100 to 150 °C nitrite can react with secondary amines to produce nitrosamines. It may create an environmental risk for example in spent solvent spills.

MAPA

The secondary amine of MAPA can form stable nitrosamine and nitramine byproducts, while the primary amine can form stable nitramine. These are the major byproducts. The work of Lepaumier et al. (2009a) indicates that diamines in the presence of carbon dioxide are likely to form condensation products with formaldehyde. However, the nitrosated and nitrated products are unstable nitrosamides or nitramides.

The reactions with NO_x can promote the formation of the relevant secondary amine by a dimerization reaction. This product has three secondary amines that are capable of forming the full range of nitrosated or nitrated byproducts. However, all of these were rated of minor importance. (Mitch 2013.) The most important degradation products are presented in Figure 5.

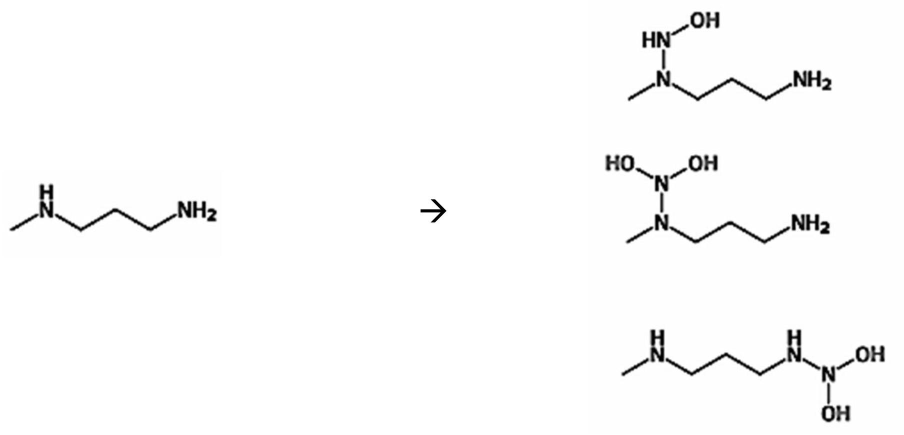

Figure 5. MAPA and its degradation products with NO_x (Mitch 2009).

DEEA

Based upon the work of Lepaumier et al. (2009a, b), dealkylation of DEEA is likely to yield secondary amine products such as N-ethylethanolamine and diethylamine. These are likely to form stable nitrosamines and nitramines. Lepaumier et al. also suggest that polymerization products of N-ethylethanolamine form a secondary amine. This can form stable nitrosated and nitrated products. The same studies suggest that piperazines are major degradation products of N-ethylethanolamine. However, the piperazines that are formed tend to have tertiary nitrogens that resist facile nitrosation or nitration. (Mitch 2009.) Some of the most common degradation products are presented in Figure 6.

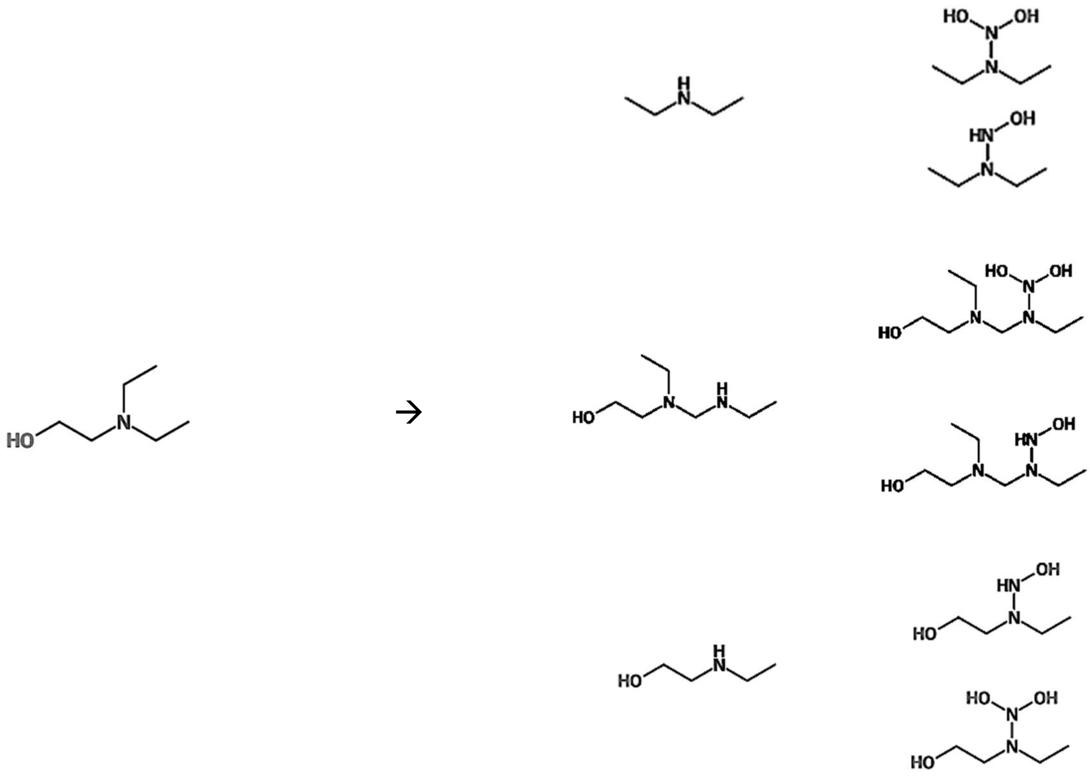

Figure 6. Degradation products of DEEA (Mitch 2009).

9.2.5 Hydrocarbons

The solubility of hydrocarbons and fixed gases on aqueous amine solutions depend on the solvent and the particular hydrocarbon species. For example, hydrogen and low molecular weight aliphatics have fairly low solubility and high molecular weight aliphatics and especially aromatic compounds (BTEX) have much higher solubility. Also the effects on the process vary. Low molecular weight hydrocarbons increase air demand and hydraulic volume in the sulphur plant and lower the sulphur recovery efficiency. On the other hand aromatics (BTEX) can lead to catalyst coking in units with acid gas feeds that are lean in H_2S. In rich feeds of H_2S and especially oxygen-enriched units temperature control problems can result. In some cases, heavy hydrocarbons in the right boiling range can be steam stripped and trapped in the overhead circuit of the stripper, leading to foaming. (Hatcher et al. 2013.)

Hydrocarbon solubility in amine treating solvents is expected to be higher than in water and the solubility depends not only on the particular amine but also on its strength. The presence of amines in the aqueous phase increases hydrocarbon solubility over that in water. The amine “salts-in” hydrocarbons. However, dissolved acid gases cause in contrary “salting-out” of hydrocarbons (and fixed gases). When acid gases are dissolved in and they react with the solvent then the ionic components formed cause high ionic strength, which further causes dissolved hydrocarbon and fixed gas concentrations to be much lower. (Hatcher et al. 2013.)

10 MODELS USED IN AQUEOUS DEEA + MAPA SYSTEM SIMULATION

Modelling can be used for predicting vapour-liquid-liquid equilibrium conditions such as compositions, phase-splitting and volume ratio between phases. Although a good thermodynamic model can give good predictions, the reactive multi-electrolyte and multi-solvent system makes the modelling difficult. (Hessen et al. 2010.)

To be able to compute all equilibrium concentrations, temperature and any partial pressure of CO_2 (up to 101 kPa or 1 atm) equilibrium constants and activity coefficients must be defined. The ratio α of absorbed CO_2 to amine can be determined from the equilibrium concentrations. The ratios of absorption and desorption can be compared to estimate the capacity of the system. The enthalpy of absorption can be calculated when the equilibrium concentrations and enthalpy associated with the formation of each species are known. Also the enthalpies of desorption can be determined. The predicted values can be compared with the experimentally determined ones. (McCann et al. 2008.)

For the system of DEEA + MAPA the refined electrolyte-NRTL (e-NRTL) model and extended UNIQUAC models have been fitted based on the equilibrium data of the individual components. Both models have been applied to several amine systems and also for the system of loaded aqueous DEEA + MAPA solvent to calculate the activity coefficient of the liquid phase. The equilibrium, kinetic and physical property data collected for the mixed system has been used to develop a thermodynamic model that is used in the in-house software CO2SIM. (Liebenthal et al. 2013., Svendsen 2012.) Arshad (2013a) has used the Soave-Redlich-Kwong equation of state to calculate vapour phase fugacity coefficients for phase change solvents.

The electrolyte thermodynamic model of an extended UNIQUAC to calculate liquid-phase activity coefficients is the original UNIQUAC with extended Debye-Hückel term (Arshad 2013a). Also e-NRTL is completed with the Pitzer-Debye-Hückel term and the Born term as it only accounts for the short term interactions. The Pitzer-Debye-Hückel term accounts for the long range Coulombic interactions and the Born term for the change in chemical potential when the relative permittivity of the solvent changes. (Hessen et al. 2010.) Pinto et al. (2014) have used the model to calculate the activity coefficients for the species of the solution in a pilot experiment. The model gives good predictions for the tertiary system and therefore the method is used also for a quaternary system. The correlation is also expected to give a good fit for the vapour-liquid-liquid equilibrium within the experimental data.

UNIQUAC, NRTL and UNIFAC are activity coefficient models that can be used to define phase equilibrium in situations that form two liquid phases. The nonrandom two-liquid (NRTL) equation is based on the principal of local concentrations. UNIFAC is based on UNIQUAC but is not as accurate. It can be used for preliminary estimation if experimental data is missing. For example, it gives good predictions for the existence of two liquid phases. (Frank et al. 2008.)

11 SCALE-UP

Scaling up a reactive process is challenging as the laboratory equipment capacities are a lot different of what can be achieved on large scale-up using bigger commercial equipment. The target is not only to model the capture system but to be able to extend to the entire power plant to evaluate its performance. Most data found from the literature for the DEEA + MAPA system is on laboratory scale. Pinto et al. (2013) have built a pilot plant to study the system and Liebenthal et al. (2013) and Svendsen (2012) have simulated the plant and the regeneration heat requirements. Within the iCap project it is estimated that a full-scale deployment is possible by 2015-2016.

When it comes to the stripper design Liebenthal et al. (2013) has studied that the lowest heat duty does not lead to the lowest efficiency penalty of the overall process. It is important not only to optimize the stripper or the capture unit but to consider the whole process. The standard amine systems are used to compare the relative operating costs of the new system and to evaluate the overall economics. The results for the energy consumption are given as a function of the liquid/gas ratio. The liquid to gas ratios are compared with

$$\frac{L}{G} = \frac{m_{\mathrm{liquid},1}}{Q_{\mathrm{gas},1}} = \frac{m_{\mathrm{liquid},2}}{Q_{\mathrm{gas},2}} \tag{19}$$

where
L/G is liquid to gas ratio [kg/m^3]
$m_{\mathrm{liquid},1}$ is the mass flow of the liquid 1 [kg/h]
$m_{\mathrm{liquid},2}$ is the mass flow of the liquid 2 [kg/h]
$Q_{\mathrm{gas},1}$ is the volumetric flow of the gas 1 [m^3/h]
$Q_{\mathrm{gas},2}$ is the voumetric flow of the gas 2 [m^3/h]

Table 4 presents the operational parameters of a pilot plant of Pinto (2014). The liquid to gas ratio is around 0.035 kg/m^3, which is quite small when compared to the pilot process of activated methyldiamine (6.95 kg/m^3) or MEA (1.6 kg/m^3) in the study of Mustonen (2013). The ratio is chosen for one of the cases for the calculations of the mass transfer and decanter dimensioning of this thesis.

Table 4. The operational parameters of a CO_2 capture pilot plant with DEEA + MAPA system (Pinto et al. 2014).

Pinto et al. (2014)	
Absorber diameter : Packing height [m]	0.15 : 4.23
Desorber diameter : Packing height [m]	0.10 : 3.57
Liquid flow into the absorber [kg/h]	2.7–3.3
Gas flow [m^3/h]	88–90
Liquid to gas ratio [kg/m^3]	0.031-0.037
Reboiler duty [kWh]	4.3–9.1
Produced CO_2 [kg/h]	2.0–13.0
Reboiler temperature [°C]	107–117
Reboiler pressure [bar]	1.75

11.1 Process feeds

11.1.1 Flue gas feed

A typical composition of a coal fired power plant of 565 MW is presented in Table 5 as volumetric and molar fraction. Also the mass and molar flows of each component are shown. 80% of nitrogen oxides, 85-90% of sulphur oxides and 99.9% of dust are removed before the capture unit (Mustonen 2013).

Table 5. The typical flue gas composition of coal fired power plant in mole and dry volume fraction and also the mass and volumetric flow rates of the flue gas. (Mustonen 2013).

Flue gas	Dry volume fraction [%]	Mole fraction [%]	Mass flow *m* [kg/s]	Molar flow *N* [kmol/s]
CO_2	14.200	12.7312	118.80000	2.699
H_2O	0.000	10.9434	41.80000	2.320
N_2	79.800	71.4813	424.50000	15.154
O_2	5.000	3.9764	30.33000	0.843
Ar	0.952	0.8538	7.22000	0.181
NO_x	0.007	0.0066	0.06430	1.398E-03
SO_3	0.001	0.0008	0.01350	1.690E-04
SO_2	0.007	0.0065	0.08880	1.386E-06
total	99.960	100	622.81660	21.199

In the study of Liebenthal et al. (2013) the flue gas downstream from flue gas desulphurisation has the temperature of 50 °C and pressure of 1.018 bar. In the laboratory experiments for CO_2 absorption with DEEA + MAPA system the temperature has been set to 25 °C (Ciftja et al. 2013c) or 40 °C (Arshad et al. 2013b).

The amount of flue gas from the power plant is given in mass flow as a function of time. To compare the liquid to gas flow ratios the volume flow per hour is needed. It can be calculated with the formula

$$Q_i = \frac{m_i}{\rho_i} \tag{20}$$

where ρ_i is the density of the component i [kg/m^3]
m_i is the mass flow of the component i [kg /h]
Q_i is the volume flow of the component i [m^3/h]

and the molar flow that is needed to determine the loading of CO_2 can be computed with

$$N_i = \frac{m_i}{M_i} \tag{21}$$

where N_i is the molar flow of the component i [mol/h]
M_i is the molar mass of the component i [g/mol].

The density of the flue gas is calculated with

$$\rho_{\mathrm{TOT}} = \rho_i p_i = \rho_i x_i P \tag{22}$$

where ρ_{TOT} is the total density of the mixture [kg/m^3]
ρ_i is the density of the component i [kg/m^3]
p_i is the partial pressure of the component i [bar]
P is the total pressure [bar]
x_i is the molar ratio of the component i.

When the temperature is changed the density of a fluid can be calculated with

$$\rho_{1\mathrm{T}} = \frac{\rho_{0\mathrm{T}}}{1 + \beta(t_1 - t_0)} \tag{23}$$

where ρ_{1T} = final density (kg/m^3)
ρ_{0T} = initial density (kg/m^3)
β = volumetric temperature expansion coefficient (m^3/m^3 °C)
t_1 = final temperature (°C)
t_0 = initial temperature (°C).

As presented in (iDEVO 2010), when ρ_0 is the density at 0 °C at 1 bar for flue gas the formula becomes

$$\rho_{1T} = \frac{273\rho_{0T}}{(t_1 - 273)} \tag{24}$$

11.1.2 Solvent feed

To achieve a certain loading α for a known amount of CO_2 in the flue gas feed the minimum liquid feed flow must be determined. The molar amine flow is

$$N_{\mathrm{amine}} = \frac{N_{\mathrm{CO2}}}{\alpha} \tag{25}$$

where N_{amine} is the amine molar flow [mol/h]
N_{CO2} is the CO_2 molar flow [mol/h].

The mass flows of DEEA, MAPA and H_2O can then be calculated with

$$m_i = x_i M_i N_{\mathrm{TOT}} \tag{26}$$

where N_{TOT} is the total molar flow of the solvent feed [mol/h].

The amount of DEEA and MAPA are given in weight percent in the literature. It can be used to calculate the molar ratio of the components

$$x_i = \frac{\frac{w_i}{M_i}}{\frac{w_{\mathrm{TOT}}}{M_{\mathrm{TOT}}}} \tag{27}$$

where w_t is the mass ratio of the component i

w_{TOT} is the total mass ratio
M_{TOT} is the total molar mass.

Finally the total mass flow of the solvent feed is

$$m_{\text{solvent}} = m_{\text{DEEA}} + m_{\text{MAPA}} + m_{\text{H2O}} \tag{28}$$

where
m_{solvent} is the total mass flow of the feed [kg/h]
m_{DEEA} is the mass flow of DEEA [kg/h]
m_{MAPA} is the mass flow of MAPA [kg/h]
m_{H2O} is the mass flow of H_2O [kg/h].

11.1.3 Decanter feed

The liquid outlet flow from the absorber is then led to the gravity settler. The liquid outlet flow consists of the loaded solvent

$$m_{\text{OUT}} = m_{\text{solvent}} + m_{\text{CO2}} \tag{29}$$

where
m_{OUT} is the outlet flow of the loaded solvent from the absorber [kg/h]
m_{CO2} is the mass flow of the CO_2 feed to the absorber [kg/h].

With the increasing CO_2 partial pressure and loading the volume ratio of the heavy phase to light phase increases (Arshad 2014., Monteiro 2011). To determine the distribution in mass flow the mass ratio can be calculated with

$$w_1 = \frac{\rho_1 V_1}{\rho_1 V_1 + \rho_2 V_2} \tag{30}$$

where
w_1 is the mass ratio of the phase 1
ρ_1 is the density of the phase 1 [kg/m^3]
ρ_2 is the density of the phase 2 [kg/m^3]
V_1 is the volume of the phase 1 [m^3]
V_2 is the volume of the phase 2 [m^3].

11.2 Dimensioning of a decanter

Decanters (or gravity settlers) are used to separate liquids that have a sufficient difference in the density so that the droplets settle readily. The decanter tank is designed to give a sufficient residence time for the droplets of the dispersed phase to rise or settle to the interphase between the phases and then coalescence. Three zones can be identified: clear heavy liquid, separating dispersed liquid (dispersion zone) and clear light liquid. Normally decanters are designed for continuous process but a batch process can use the same principles. The most used vessel shape is cylindrical and it is often also the cheapest one. (Sinnott 2005: 440.) Usually the vessel is made horizontal to have shorter travel distance to the separated phase. (Penney et al. 2012: 657.)

When dimensioning the decanter vessel the basis is that the velocity of the heavy phase must be less than settling velocity of the droplets of the light phase or the velocity of the light phase less than the settling velocity of the droplets of the heavy phase. In a plug flow velocities should be (Sinnott 2005: 442., Penney et al. 2012: 657)

$$v_{\mathrm{c}} = \frac{Q_{\mathrm{c}}}{A_{\mathrm{i}}} < v_{\mathrm{d}} \tag{31}$$

where v_c is continuous phase cross-flow velocity [m/s]
v_d is the settling velocity of the dispersed phase droplets with diameter d [m/s]
Q_c is volumetric flow rate of the continuous phase [m^3/s]
A_i is area of the interface [m^2].

Which phase is continuous and which one dispersed makes a significant difference as only the continuous phase viscosity is considered (Sinnott 2005: 442). The dispersed phase can be identified with the factor (Penney et al. 2012: 657)

$$c = \frac{Q_{\mathrm{LP}}}{Q_{\mathrm{HP}}}\left(\frac{\rho_{\mathrm{LP}}\mu_{\mathrm{HP}}}{\rho_{\mathrm{HP}}\mu_{\mathrm{LP}}}\right)^{0.3} \tag{32}$$

where Q_{LP} is the volumetric flow of the light phase [m^3/s]
Q_{HP} is the volumetric flow of the heavy phase [m^3/s]
ρ_{HP} is the density of the heavy phase [kg/m^3]
ρ_{LP} is the density of the light phase [kg/m^3]

μ_{LP} is the viscosity of the light phase [Ns/m^2]
μ_{HP} is the viscosity of the heavy phase [Ns/m^2].

If the factor is (Selker & Schleicher 1965., Penney et al. 2012)

<0.3	the light phase is always dispersed,
0.3-0.5	the light phase is probably dispersed,
0.5-2.0	phase inversion is probable and design made for the worst case,
2.0-3.3	heavy phase is probably dispersed,
>3.3	heavy phase is always dispersed.

11.2.1 Diameter of the decanter

The method needs trial-and-error calculations to be solved (Purarelli 1994: 470). The diameter D and the length L of the decanter are chosen for the calculations. Usually the L/D ratio is three or more (Penney et al. 2012:657). To simplify the calculations it is assumed that the decanter has only one layer between the light and heavy phase. In reality there are two of them and the dispersion zone in between. (Purarelli 1994: 470.) A picture of a horizontal vessel and its dimensions can be seen in Appendix 2, Figures 7 and 8.

As given in Finlayson & Biegler (2008) the volume of the vessel can be calculated with the following equation

$$V = \pi r^2 L \tag{33}$$

where
V is the volume of the separator vessel [m^3]
L is the length of the separator [m]
r is the separator radius $r=D/2$ [m].

Next the distance of the interface from the middle must be chosen. The position of the interface should not extend to the bottom or the top of the vessel. In the design a value of 10% of the decanter diameter is often applied. According to (Sinnott 2005: 443) the width of the interface is then computed with

$$L_{\mathrm{i}} = 2\sqrt{r^2 - H_{\mathrm{i}}^2} \tag{34}$$

where L_{i} is the width of the interface [m]
H_{i} is the height if the interface from the middle of the vessel [m]

and the area of the interface is

$$A_{\mathrm{i}} = L_{\mathrm{i}}L \tag{35}$$

where A_{i} is the area of the interface [m^2].

The height of the heavy phase is the distance of the interface from the bottom of the vessel

$$H_{\mathrm{HP}} = r + H_{\mathrm{i}} \tag{36}$$

where H_{HP} is the height of the heavy phase [m]

and the height of the light phase is

$$H_{\mathrm{LP}} = D - H_{\mathrm{HP}} \tag{37}$$

where H_{LP} is the height of the light phase [m].

As presented by Finlayson & Biegler (2008) the cross-sectional surface areas of the vessel and for the light and heavy phases can be calculated with

$$A = \pi r^2 \tag{38}$$

where A is the cross-sectional surface area [m^2]

$$A_{\mathrm{LP}} = A_{\mathrm{S}} - A_{\mathrm{k}} = \mathrm{acos}\left(\frac{H_{\mathrm{i}}}{r}\right) r^2 - H_{\mathrm{i}}L_{\mathrm{i}} \tag{39}$$

where A_{LP} is the cross-sectional surface area of the light phase [m^2]
A_{S} is the area of the sector [m^2]
A_{k} is the area of the triangle [m^2]

$$A_{\mathrm{HP}} = A - A_{\mathrm{LP}} \tag{40}$$

where A_{HP} is the cross-sectional surface area of the heavy phase [m^2].

Now the volumes of the heavy and light phases are calculated with

$$V_{\mathrm{LP}} = A_{\mathrm{LP}} L \tag{41}$$

where V_{LP} is the volume of the light phase [m^3]

$$V_{\mathrm{HP}} = A_{\mathrm{HP}} L \tag{42}$$

where V_{HP} is the volume of the heavy phase [m^3].

11.2.2 Settling velocity

The separation of the droplet is dependent on the difference in densities of the two phases, the viscosity of the continuous phase and the droplet size and shape. The settling velocity of the droplets can be determined with the Stoke’s law

$$v_{\mathrm{d}} = \frac{d^2 g(\rho_{\mathrm{d}} - \rho_{\mathrm{c}})}{(18\mu_{\mathrm{c}})} \tag{43}$$

where d is the droplet diameter [m]
μ_{c} is the viscosity of the continuous phase [Ns/m^2]
g is the gravitational acceleration, 9.81 m/s^2
ρ_{c} is the density of the continuous phase [kg/m^3]
ρ_{d} is the density of the dispersed phase [kg/m^3].

The equation is used to calculate the settling velocity for a droplet maximum size of 150 μm, which is below the droplet sizes normally found in decanter feeds (Sinnott 2005:

442). Usually the minimum droplet diameters are in the range of 500-5000 μm. Very few droplets are smaller than 500 μm in a turbulent pipeline flow (Penney et al. 2012).

Two terminal settling velocities can be calculated: the velocity of heavy phase droplets settling out of the light phase and the velocity of light phase droplets settling out of the heavy phase. If the factor c value is between 0.5-2.0 and the dispersed phase is unknown, the design is made for the worst case. To maintain a realistic interface level in the settler the maximum value for the settling time is determined. However, the fastest settling velocity should be no more than 0.004 m/s or 120% of the slowest settling velocity times the ratio of the least viscous phase flow rate to the most viscous phase flow rate, whichever is smaller (Sinnott 2005:442., Abernathy 1993: 129).

11.2.3 Settling time

Abernathy (1993: 132) states that the settling velocity of the dispersed phase can be used to calculate the time the dispersed phase particle takes to rise through the continuous phase

$$t_{\mathrm{d}} = \frac{H_{\mathrm{c}}}{v_{\mathrm{d}}} \tag{44}$$

where t_{d} time for the drop to rise or fall [s]
H_{c} is the height of the continuous phase [m].

When it is not clear which phase is dispersed, the time that is longer for the rise or fall is chosen for the further calculations.

11.2.4 Residence time

The residence time of the continuous phase must be checked. It should be less than the settling time of the dispersed drops to make sure it is long enough for good separation. If not the chosen diameter and length should be revised. According to Abernathy (1993: 131) the residence time of the light phase can be calculated with the formula

$$t_{\mathrm{c}} = \frac{V_{\mathrm{c}}}{Q_{\mathrm{c}}} \tag{45}$$

where t_{c} is the residence time of the continuous phase [s]
V_{c} is the volume of the continuous phase [m^3].

Also the diameter of the droplet must be accurately chosen as it affects the settling time. Spellman & Whiting (2005:219) presents that the minimum size of the settling droplet that can be collected with 100% efficiency can be calculated from the Equation (43) by using the overflow velocity of the continuous phase

$$d_{\mathrm{min}} = \frac{v_{\mathrm{i}} g(\rho_{\mathrm{d}} - \rho_{\mathrm{c}})}{(18\mu_{\mathrm{c}})} \tag{46}$$

where d_{min} is the minimum diameter of the settling droplet [m]
v_{i} is the overflow velocity of the continuous phase [m/s]

$$v_{\mathrm{i}} = \frac{Q_{\mathrm{c}}}{A_{\mathrm{i}}} \tag{47}$$

The chosen droplet diameter should be bigger than the minimum diameter.

11.2.5 Reynolds number

The rise or fall of the liquid droplets can be interfered by lateral flow of the liquid (Frank et al. 2008., Hooper & Jacobs 1979). The effectiveness of the separation can be estimated with the Reynolds number

$$Re = \frac{v_{\mathrm{c}} \rho_{\mathrm{c}} D_{\mathrm{h}}}{\mu_c} \tag{48}$$

where v_{c} is the continuous phase cross-flow velocity [m/s]
D_{h} is the hydraulic diameter of the continuous phase layer (given by four times the flow area divided by the perimeter of the flow channel including the interface) [m].

In the work of Couper et al. (2012) the hydraulic diameter of the phase is calculated with the formula

$$D_{\mathrm{h}} = \frac{4A_{\mathrm{c}}}{L_{\mathrm{i}} + S_{\mathrm{c}}} \tag{49}$$

where D_{h} is the hydraulic diameter [m]
A_{c} is the flow area of the continuous phase [m^2]
S_{c} is the perimeter of the continuous phase cross-sectional area [m]

for which the arc of light and heavy phases can be calculated with

$$S_{\mathrm{LP}} = \frac{2}{2\pi} acos\left(\frac{H_{\mathrm{i}}}{r}\right) 2\pi r^2 \tag{50}$$

where S_{LP} is the arc of the light phase cross-sectional area [m]

$$S_{\mathrm{HP}} = 2\pi r - S_{\mathrm{LP}} \tag{51}$$

where S_{HP} is the arc of the heavy phase cross-sectional area [m].

If the Reynolds number is under 5000 the design is good. With 5000-20 000 there is some hindrance. With Re from 20 000 to 50 000 there exists major problems and above that poor separation can be expected (Frank et al. 2008., Penney et al. 2012: 657).

11.3 Other separation methods

The separation rate can be enhanced by shortening the path through which the droplets need to rise or fall or by increasing their diameter. Both can be achieved by forcing the flow through a parallel flat of crimped plates, tower packing or a mass of packed fibres. (Couper et al. 2012.) These coalescers can be used for separation of finely dispersed droplets. The medium works by holding up the dispersed droplets long enough so that they grow sufficiently to settle. Coalescing filters can be used to separate small quantities of dispersed liquids from large throughputs. The use of plates increases the interfacial area per unit volume and reduces turbulence, which gives the effect of several smaller separators connected in parallel. Coalescence can also be induced electrically, which is used for desalting crude oils and similar applications. (Sinnott 2005: 445.)

Sedimentation centrifuges can be used in difficult separations, where simple gravity settling does not give separation good enough or when settling times are long. Centrifuges can be used even for small density differences between the liquids and it breaks the emulsion that might form. Normally a bowl or a disc centrifuge is applied. (Sinnott 2005: 446.) Very fine dispersions can be separated with the disk-type centrifuges with capacity of 1.32-1320 m^3/h (Couper et al. 2012).

Hydrocyclones give a mild centrifugal action and they are used for some liquid-liquid separations. In general their effectiveness for liquid-liquid separation is not good. (Couper et al. 2012., Sinnott 2005: 446.)

11.4 Stripper

The feed to the stripper is the heavy phase flow rate from the separator. In the higher temperatures of the stripper to release carbon dioxide the vapour pressure of the solvent increases and also a part of the solvent exits with the gas flow. The amount of solvent can be calculated with the Amagat’s law for additive volume

$$Q_{\mathrm{S,G}} = \frac{Q_{\mathrm{gas}}\, p_{\mathrm{S}}}{p_{\mathrm{TOT}}} \tag{52}$$

where $Q_{\mathrm{S,G}}$ is the volume flow of the solvent in the gas outlet flow [m^3/h]
Q_{gas} is the volume flow of the gas outlet from the stripper [m^3/h]
p_{S} is the partial pressure of the solvent [kPa]
p_{TOT} is the total pressure of the stripper [kPa].

The same law is used to calculate the volume of the gas phase in the stripper

$$Q_{\mathrm{gas}} = \frac{Q_{\mathrm{CO2}} p_{\mathrm{CO2}}}{p_{\mathrm{TOT}}} \tag{53}$$

where Q_{CO2} is the volume flow of CO_2 in the gas outlet flow [m^3/h]
p_{CO2} is the partial pressure of CO_2 [kPa].

The partial pressure of the solvent can be calculated with the Raoult's law

$$p_i = P_i^o x_i \tag{54}$$

where p_{i} is the partial pressure of the component i [kPa]
$P^{\mathrm{o}}_{\mathrm{i}}$ is the vapour pressure of the component i [kPa]
x_{i} is the mole ratio of the component i in the mixture

and total pressure with the Dalton's law

$$p_{\mathrm{TOT}} = \sum p_i \tag{55}$$

However, these laws mostly apply only for ideal gases and do not consider the interactions in the gas.

12 PROCESS CALCULATIONS

Four different cases of solvent flow rate in the capture unit are investigated to have an estimation of dimensions of a capture unit designed for a coal fired power plant of 565 MW (Mustonen 2013). Also the experimental values of viscosities and densities are used to size a gravity settler that separates the two liquid phases. Atmospheric pressure and temperature of 25 °C are assumed. Degradation and vaporisation of the solvent or impurities are not taken into consideration.

12.1 Flue gas flow rate

The composition of the flue gas given by Mustonen (2013) is assumed (Table 6). To calculate the flue gas mass flow the density of the flue gas has been calculated with Equation (22). The densities of different components and the total density of the flue gas are given also in Table 6.

Table 6. Density of the flue gas and its components calculated with the Equation (22).

Flue gas	Mole fraction [%] (Mustonen 2013)	Density ρ_{0T} [kg/Nm^3] at 0 °C, 1 bar (iDEVO AB 2010)	Density in the flue gas ρ_{1T} [kg/Nm^3]
CO_2	12.7312	1.977	0.252
H_2O	10.9434	0.804	0.088
N_2	71.4813	1.25	0.894
O_2	3.9764	1.43	0.057
Ar	0.8538	1.25	0.011
NO_x	0.0066	-	-
SO_3	0.0008	-	-
SO_2	0.0065	2.927	0.000
Total	100	-	1.301

When the final density of the flue gas is 1.301 kg/m^3 at 0 °C with the Equation (24) the density in 25 °C for flue gas is 1.192 kg/m^3 and for CO_2 1.811 kg/m^3.

Mustonen (2013) is giving the flow rates of flue gas and it’s components as mass flow. To compare both loading and L/G ratio the volumetric flow of the flue gas and carbon dioxide is computed with the Equation (20). The flow rates are presented in Table 7.

Table 7. The flow rates of flue gas and carbon dioxide.

Flue gas into absorber	Flue gas	CO_2
Flue gas inlet flow [kg/h] (Mustonen 2013)	2242139.76	427680.00
Inlet flow [m^3/h] (Eq. 20)	1881329.84	267166.77
Inlet flow [mol/s] (Mustonen 2013)	21199.00	2699.00

12.2 Solvent flow rate

The concentrations of 5 M DEEA and 2 M MAPA have shown good results and is used in other studies for the solvent (Ciftja et al. 2013c., Arshad et al. 2014) and it is also applied here. The composition in mass percent is presented in Table 8. The amount of water is calculated by subtracting the amount of amine from 100%. The properties of MAPA and DEEA are gathered in Table 9.

Table 8. Composition of the solvent in mass fraction.

Amine flow into absorber	Mass fraction [%]
H_2O	17.4
5 M DEEA (Arshad et al. 2013b)	63.5
2 M MAPA (Arshad et al. 2013b)	19.1

Table 9. The properties of MAPA and DEEA (Sigma-Aldrich 2013a, b).

	MAPA 3-(methylamino)propylamine or 3-amino-1-methylaminopropane	DEEA 2-(diethylamino)ethanol or NN-(diethylethanolamine)
	Clear and colorless liquid	Clear liquid with pale yellowish colour
Molecular formula	$C_4H_{12}N_2$	$C_6H_{15}NO$
Molecular weight [g/mol]	88.15	117.19
Freezing point [°C]	-72	-70
Boiling point [°C]	140	161
Solubility in water	completely	completely
Density [g/ml] at 25 °C	0.844	0.884
pH at 20 °C	11.5	-
Vapour pressure 20 °C [kPa]	0.5	0.1

The four different cases of solvent mass flow are presented in Table 10. More detailed calculations can be found in the Appendix 3, Table 15. The first three cases are based on the minimum solvent feed that is required to achieve a certain loading. Case 1 is chosen based on the loading of 0.196 achieved in the experimental part and thus the liquid to gas ratio is adjusted to achieve the loading. The second case is based on the loading of 0.45 that is achieved with the given CO_2 partial pressure and is resulting in two phases (Arshad et al. 2014). The case 3 is with the loading of 1, which is high enough that only one phase exists (Arshad et al. 2013b). The fourth case is based on the liquid-gas ratio 0.037 of the pilot plant studied by Pinto et al. (2014). However, to capture all CO_2 it is calculated that the loading of 18.6 would be required (Equation 18), which is not here realistic.

The solvent feed is calculated with the Equations (25)-(28). For the first three cases it is assumed that carbon dioxide is absorbed totally. For the case 4 the high loading of 1.2 is chosen. Although the loading is high, with the given liquid to gas ratio the amount of CO_2 absorbed would be only 14.7%, which is not enough as the target is at least 90%. The outlet flow rate for all the cases is calculated by adding the amount of absorbed CO_2 into the amount of solvent. The possible solvent loss with the flue gas outlet stream is not taken into account.

As the solvent forms two liquid phases the distribution of these phases is computed for the decanter calculations. Arshad et al. (2013b, 2014) have studied loading and forming of two phases and Monteiro et al. (2011) gives the volume distribution of the lower to upper phase in 40 °C, which are used to estimate the solvent phase distribution for different loadings. In the case 1 the volume distribution ratio of the lower to upper phase is set to 0.45 and in the case 2 the mass ratio is estimated to be 50:50 at 25 °C. For the cases 3 and 4 the loading is so high that formation of one phase is assumed (Arshad et al. 2013b).

The solvent flow rates seem to be quite big. However, when the liquid to gas ratio is calculated with the Equation (19) it is found to be in the same scale when compared with the liquid to gas rates from the study of Mustonen (2013). It is 6.33 kg/m^3 (α = 0,19) for activated MDEA and 1.5 kg/m^3 for MEA (α = 0,11).

Table 10. The flow rates of the solvent, loading and liquid to gas ratio for different cases.

	Case 1	Case 2	Case 3	Case 4
Loading (Eq. 18)	0.196	0.45	1.00	18.57 (1.2)
Liquid to gas ratio |kg/m^3] (Eq. 19)	3.474	1.513	0.681	0.037
Flue gas inlet flow [m^3/h] (Mustonen, 2013)	1 881 330	1 881 330	1 881 330	1 881 330
Solvent inlet flow [kg/h] (Eqs. 25-28)	6 535 455	2 846 554	1 280 949	68 982
Solvent outlet flow [kg/h] (Eq. 29)	7 019 333	3 330 431	1 764 827	131 803
Outlet flow upper phase [kg/h] (Eq. 30)	2 633 100	1 631 457	-	-
Outlet flow lower phase [kg/h] (Eq. 30)	4 386 232	1 698 975	-	-

12.3 Decanter dimensions

The experimental data of Uusi-Kyyny (2014) for viscosities and densities is used to make a rough dimensioning of a gravity settler. It is more relevant for case 1 with the same loading but for case 2 the effect of change in the loading of the solvent to viscosity and density is not considered. It is assumed that the feed flow consists of two liquid phases and no gas phase. For the decanter dimensioning only cases 1 and 2 are used due to the presence of two liquid phases. The decanter is dimensioned with the trial-and-error calculations. The diameter, length, height of the dispersed phase and the droplet size are chosen and changed until they fulfil the requirements.

First it is determined which phase is dispersed by using Equation (32). With the factor c value of 7.9 for the case 1 and 4.9 for the case 2 it can be identified that the heavy phase is dispersed.

By calculating the minimum droplet size with Equation (46) it can be checked that it is smaller than the set droplet diameter. In other case the set dimension and length is changed. However, the maximum droplet diameter of 0.00015 m for the Stoke's law was found to give highly unrealistic dimensions for the decanter. In the study of Pinto et al. (2011) the observations of the formation of two liquid phases are described as similar as the formation of oily dispersed droplets in water. Based on this the size of the droplet diameter is set to 0.001 m, although the dimensions gained with it do not give as good collection efficiency. This is not beneficial as the heavy phase is dispersed which means that part of carbon dioxide do not reach the stripper but exits with the light phase. More information for the droplet size distribution is needed to have more accurate estimations of the separation efficiency. For small droplets a coalescer could be applied.

The settling time of the heavy phase droplets must be smaller than the residence time of the light phase to assure a good separation and it is set by changing the diameter and length. The times are calculated with Equations (44) and (45). The length and diameter fulfilling these requirements and the results for the settling and residence times are presented in Table 11. Even now the settling time is over 10 minutes. It is quite long for a continuous process, which is why techniques to speed up the separation should be considered.

Finally, by calculating the Reynolds number with Equation (48) the effectiveness of the separation can be estimated. The Reynolds number of 117 for the case 1 and 113 for the case 2 indicate separation that is not distracted by turbulence. Even though the droplet size could be increased the separation requires quite enormous dimensions of the vessel especially if the loading is low. With a higher loading the flow rates would decrease and the separation vessel size could be decreased. Other dimensions and calculations of the decanter can be observed in Appendix 3, Tables 16-20.

Table 11. The dimensions of the decanter.

		Case 1	Case 2
The chosen diameter	D [m]	7.8	4.4
The chosen length	L [m]	25.1	17.8
The settling time (Eq. 44)	t_d (HP) [s]	645.6	303.5
The residence time of the light phase (Eq. 45)	t_c (LP) [s]	647.1	303.8
Reynolds number (Eq. 48)	Re	117	113

12.4 Stripper flow rate

The separated heavy phase is led to a stripper for regeneration. Assuming the separation is good 4 557 182 kg/h of loaded solvent is fed to the stripper in the case 1 and 2 349 532 kg/h in the case 2. In the literature the laboratory scale and simulation stripping temperatures range from 88-155 °C and pressure from 2 to 6 bar (Liebenthal et al. 2013., Svendsen 2012., Pinto et al. 2014). With the stripper conditions from the literature presented earlier (see appendix 1.) the reboiler duties are determined in the Table 12 for the given carbon dioxide recovery. To achieve higher CO_2 recovery the reboiler duty must be increased.

Table 12. Reboiler duties and CO_2 recovery from the stripper.

	Regeneration temperature [˚C]	Regeneration pressure [kPa]	Reboiler duty [MJ/kg]	CO_2 recovery [%]	CO_2 mole fraction in lean from stripper	Reboiler duty [MJ/h]	Reference
1	88.00	400	2.4	90	-	577 080	Liebenthal et al. 2013
2	107.00	175	2.52	-	-	-	Pinto et al. 2014
3	141.96	400	2.19917	82.37	0.0375	483 961	Svendsen 2012
4	149.38	600	2.24408	80.68	0.0409	483 712	Svendsen 2012
5	155.49	600	2.24896	87.24	0.0274	524 179	Svendsen 2012

The recovered CO_2 and the gas outlet flow composition are presented in Table 13. The flow rates were calculated with Equations (52) and (53). The same conditions are applied as in Table 12. More detailed calculations are presented in the Appendix 3, Tables 21-22. The non-ideality of the solvent is not considered, which might bring some errors. The outlet flow contains a small amount of solvent. A condenser or a washing section can be added after the stripper to separate the solvent and lead it to the lean flow.

Table 13. CO_2 and solvent outlet flow from the stripper with certain carbon dioxide recoveries.

	CO_2 outlet from stripper [m^3/h]	Case 1, solvent in gas outlet flow (Eq. 35) [m^3/h]	Total gas outlet flow (Eq. 36) [m^3/h]
1	240 450	0.32	240 450
2	-	-	-
3	220 065	0.77	220 066
4	215 550	0.30	215 550
5	233 076	0.53	233 077

13 CONCLUSIONS AND PROPOSALS FOR FURTHER STUDIES

In this study the phase change solvent system of aqueous DEEA + MAPA and its potential to reduce energy consumption of the carbon dioxide capture process was examined. The literature study shows that the energy consumption and the net efficiency penalty are remarkably lower for the solvent DEEA + MAPA than for the reference MEA. It is estimated that the potential for reducing capture plant thermal and recompression energy requirements is even 45-50%. Simulation of the heat exchanger and regenerator section has shown a potential for this system to reach regeneration heat requirement of 2 MJ/kg CO_2 depending on the CO_2 targeted removal rate per cycle. There is also a potential for regeneration at elevated pressure or reduced temperature. However it was also noticed that it is important to consider the whole process as the lowest heat duty of the reboiler did not give the best energy efficiency for the whole process. Also the pressure must be compromised for the optimal solubility, regeneration heat duty and compression energy. The results however encourage not only for the further research of the DEEA + MAPA system but also to find new solvents with the same property of forming two liquid phases and studying their potential for the acid gas capture.

The solvent flow rate was determined for certain loadings. The higher the loading the lower the liquid to gas flow rate needs to be. The L/G ratio was observed to be lower for the system of DEEA + MAPA than for activated MDEA but higher than for MEA with the same loading. Even with the higher solvent flow the energy efficiency is better than for MEA.

Good absorption capacities can be achieved with the solvent system but the increase in density and viscosity with an increasing loading must be considered. It affects for example the separation time of the two phases that has been found relatively long. The dimensions of a gravity settler to obtain good separation were calculated based on the viscosities and densities of the light and the heavy phase. The calculations show that the settling time of the dispersed droplets is long and requires major dimensions to have the residence time long enough for proper separation. More detailed measurements should be made over the viscosities and densities for different loadings and temperatures. Further studies could also be made for the use of another separation method such as centrifugal separation or the use of coalescers to enhance the separation velocity.

When applying the solvent in an industrial scale the environmental factors must be considered. Especially MAPA shows oxidative and thermal degradation problems, which are common for secondary amines, but inhibitors can be considered. On the other hand MAPA is well biodegradable. A risk of the formation of carcinogenic nitrosamines exists as secondary amines like MAPA can form them with NO_2 of the inlet flue gas. However, the lower regeneration temperatures of the DEEA + MAPA system could decrease the risk. Further studies should be made of the degradation of DEEA+ MAPA system and its behaviour with impurities. Emissions can be decreased by treating the flue gas exiting absorber or CO_2 outlet flow from the stripper.

As the volume ratio of the lower to upper phase increases with an increasing CO_2 loading, with higher loadings more solvent is in the heavy phase and is needed to be taken to the stripper. The regeneration energy required is then also increasing. On the other hand the total solvent circulation rate is smaller. At some point with the loading high enough the two phases become again one phase. Further investigations are still required to study the ratio of the two phases as a function of loading and to estimate the benefits of the lower loading and the savings in regeneration due to a lower amount of the heavy phase. The separation of the two phases makes the process more complex. If the absorption conditions would allow the high loading one option would be to run the process with one phase and without separation as the blend has relatively good absorption capacity and its regeneration requires less energy than the conventional MEA process.

Only a limited amount of data from laboratory, pilot and simulations was available for the scale up. Practical experiences of an industrial process can’t either be found to compare the results. Due to many assumptions and simplifications the validity of the results is uncertain. Although the study shows the phase change solvent system of MAPA+DEEA has potential many problems are still to be solved. Nevertheless, the study and calculations give directions for further investigations.

14 REFERENCES

Abernathy MWN (2013) Gravity settlers, design. McKetta J (Ed.) Unit operations handbook. Volume 2: Mechanical separation and materials handling. New York, Marcel Dekker Inc: 127-135.

Aleixo M, Prigent M, Gibert A, Porcheron F, Mokbel I, Jose J & Jacquin M (2011) Physical and chemical properties of DMX™ solvents. Energy Procedia 4: 148–155.

Alstom (2012) Alstom Chilled Ammonia Process selected for leading CO_2 capture plant in Romania. http://www.alstom.com/press-centre/2010/12/alstom-chilled-ammonia-process-selected-for-leading-cO2-capture-plant-in-romania/. [23.10.2013].

Aronu U, Hoff K & Svendsen H (2011) CO_2 capture solvent selection by combined absorption-desorption analysis. Chemical Engineering Research and Design 89 (8): 1197-1203.

Aroonwilas A & Veawab A (2007) Integration of CO_2 capture unit using single- and blended-amines into supercritical coal-fired power plants: Implications for emission and energy management. International Journal of Greenhouse Gas Control 1: 143-150.

Arshad M (2013a) Thermodynamics of phase change solvents. http://orbit.dtu.dk/en/publications/thermodynamics-of-phase-change-solvents(b5f2e293-abd5-4799-9373-c83f3e03b283).html. [1.11.2013].

Arshad M, Fosbøl P, Solms N, Svendsen H & Thomsen K (2013b) Heat of absorption of CO_2 in Phase Change Solvents: 2-(Diethylamino)ethanol and 3-(Methylamino)propylamine. Journal of Chemical & Engineering Data 58: 1974-1988.

Arshad M & Von Solms N & Thomsen K & Svendsen H (2013c) Heat of absorption of CO_2 in aqueous solutions of DEEA, MAPA and their mixture. Energy Procedia 37: 1532-1542.

Arshad M, Fosbøl P, von Solms N & Thomsen K (2013d) Freezing Point Depressions of Phase Change CO2 Solvents. Journal of Chemical Engineering Data 58: 1918-1926.

Arshad M, Svendsen H, Fosbøl P, Solms N & Thomsen K (2014) Equilibrium total pressure and CO_2 solubility in binary and ternary aqueous solutions of 2-(diethylamino)ethanol (DEEA) and 3-(methylamino)propylamine (MAPA). Journal of Chemical Engineering Data.

Ayala R & Perry R (2013) Systems and methods for capturing carbon dioxide. Patent US20130202517 A1.

Bacher A (2013) Extraction (Part 1). http://www.chem.ucla.edu/~bacher/. [10.2.2014].

Bailey A (2010) Interfaces. http://www.thermopedia.com/content/27/. [10.2.2014].

Barzagli F, Mani F & Peruzzini M (2010) Continuous cycles of CO_2 absorption and amine regeneration with aqueous alkanolamines: a comparison of the efficiency between pure and blended DEA, MDEA and AMP solutions by ^{13}C NMR spectroscopy. Energy and Environmental Science 3: 772-779.

Boot-Handford M, Abanades J, Anthony E, Blunt M, Brandani S, Dowell N, Fernandez J, Ferrari M-C, Gross R, Hallet J, Haszeldine S, Heptonstall P, Lyngfelt A, Makuch Z, Mangano E, Porter R, Pourkashanian M, Rochelle G, Shah N, Yao J & Fennell P (2013) Carbon capture and storage update. Energy & Environmental science 7: 130-189.

Brakstad O, Lauritsen K & Mejdell T (2013) Biodegradation and ecotoxicity testing of solvent systems. http://icapco2.org/0/19/eu-ccs-workshop-antwerp/. [15.1.2014].

Cadours R, Carrette P-L, Boucot P (2012) Method of deacidizing a gas with a fractional regeneration absorbent solution with control of the water content of the solution. Patent. US 8206489 B2.

Chapel D, Mariz C & Ernest J (1999) Recovery of CO_2 from flue gases: Commercial trends. http://www.netl.doe.gov/publications/proceedings/01/carbon_seq/2b3.pdf. [20.1.2014].

Ciftja A, Hartono A & Svendsen H (2013a) ^{13}C NMR as a method species determination in CO_2 absorbent systems. Internal Journal of Greenhouse Gas Control 16: 224-232.

Ciftja A, Hartono A & Svendsen H (2013b) Carbamate formation in aqueous diamine–CO_2 systems. Energy Procedia 37: 1605 – 1612.

Ciftja A, Hartono A & Svendsen H (2013c) Experimental study on phase change solvents in CO_2 capture by NMR spectroscopy. Chemical Engineering Science 102: 378-386.

Couper J, Penney W & Fair J (2012) Chemical process equipmen, 3rd edition: Process vessels: Liquid-liquid separators. Oxford: Butterworth-Heinemann.

Darde V, Thomsen K, van Well W & Stenby E (2009) Chilled ammonia process for CO_2 capture. Energy Procedia 1: 1035-1042.

Donaldson T & Nguyen Y (1980) Carbon dioxide reaction kinetics and transport in aqueous amine membranes. Industrial & Engineering Chemistry Fundamentals 19 (3): 260-266.

Eide-Haugmo I, Brakstad O, Hoff K, Sørheim K, Silva E & Svendsen H (2009) Environmental impact of amines. Energy Procedia 1: 1297-1304.

Eide-Haugmo I, Lepaumier H, Einbu A, Vernstad K, Da Silva E & Svendsen H (2011) Chemical stability and biodegradability of new solvents for CO_2 capture. Energy Procedia 4, 1631–1636.

Finlayson B & Biegler L (2008) Mathematics. Green D & Perry R (Eds.) Perry's chemical engineers' handbook, eighth edition. United States of America, McGraw-Hill Companies Inc: 3.

Francisco M, van den Bruinhorst A, Zubeir L, Peters C & Kroon M (2013) A new low transition temperature mixture (LTTM) formed by choline chloride + lactic acid : characterization as solvent for CO_2 capture. Fluid Phase Equilibria, 340: 77-84.

Frank T, Dahuron L, Holden B, Prince W, Seibert A & Wilson L (2008) Liquid-liquid extraction and other liquid-liquid operations and equipment. Green D & Perry R (Eds.) Perry's chemical engineers' handbook, eighth edition. United States of America: McGraw-Hill Companies Inc: 15.

Gary J & Handwerk G (2001) Petroleum refining: Technology and economics. Fourth edition. New York: Marcel Dekker.

Haar, L, Gallagher J & Kell G (1984) NBS/NRC Steam Tables. New York: Hemisphere Publishing Corp.

Hartono A, Saleem F, Arshad M, Usman M & Svendsen H (2013) Binary and ternary VLE of the 2-(diethylamino)-ethanol (DEEA)/3-(methylamino)-propylamine (MAPA)/water system. Chemical Engineering Science 101: 401–411.

Hatcher N, Jones C & Weiland R (2013) Hydrocarbon and Fixed Gas Solubility in Amine Treating Solvents: A Generalized Model. http://www.ogtrt.com/files/publications/LRGCC_2013_HC_Solubility_Manuscript-0.pdf. [29.1.2014].

Herzog H, Meldon J & Hatton A (2009) Advanced post-combustion CO_2 capture. https://mitei.mit.edu/system/files/herzog-meldon-hatton.pdf. [1.11.2013].

Hessen E, Haug-Warberg T & Svendsen H (2010) The refined e-NRTL model applied to CO_2– H_2O –alkanolamine systems. Chemical Engineering Science 65 (11): 3638–3648.

Hu L (2009) Phase transitional absorption method. Patent. US 7541011 B2.

iCap (2011) Innovative CO_2 capture: Project overview. http://www.sintef.no/project/TCCS6/Presentations/D2/03%20ICAP%20Project%20Overview%20updated.pdf. [28.1.2014].

iCap (2013) Characterization of liquid-liquid systems. http://icapco2.org/0/16/seminar-st-etienne/files/WP1-Characterization_of_Liquid-Liquid_systems.pdf. [4.2.2014].

iDEVO AB (2010) Density of flue gases. http://www.idevo.se/index.php?option=com_content&view=article&id=60:densitet-a-taethet&catid=36:formelsamling&Itemid=63&lang=en. [5.3.2014].

IPCC (2005) Carbon dioxide capture and storage: Special report of the intergovernmental panel on climate change. https://www.ipcc.ch/publications_and_data/_reports_carbon_dioxide.htm. [1.12.2013].

IPCC (2012) Renewable Energy Sources and Climate Change Mitigation, Special Report of the Intergovernmental Panel on Climate Change. http://srren.ipcc-wg3.de/report. [1.12.2013].

Katritzky A, Meth-Cohn O & Rees C (1995) Comprehensive organic functional group transformations. Roberts S (Ed.) Volume 1: Synthesis: Carbon with no attached heteroatoms. Oxford. Elsevier science ltd: 1-426.

Kim I (2009) Heat of reaction and VLE of post combustion CO_2 absorbents. PhD thesis. Norwegian University of Science and Technology.

Kim I & Svendsen H (2007) Heat of Absorption of Carbon Dioxide (CO_2) in Monoethanolamine (MEA) and 2-(Aminoethyl)ethanolamine (AEEA) Solutions. Industrial & Engineering Chemistry Research 46 (17): 5803–5809.

Kim I & Svendsen H (2011) Comparative study of the heats of absorption of post-combustion CO_2 absorbents. International Journal of Greenhouse Gas Control 5 (3): 390-395.

Kladkaew N, Idem R, Tontiwachwuthikul P & Saiwan C (2011) Studies on corrosion and corrosion inhibitors for amine based solvents for CO_2 absorption from power plant flue gases containing CO_2, O_2 and SO_2. Energy Procedia 4: 1761–1768.

Knudsen J, Jensen JN, Vilhelmsen PJ & Biede O (2009) Experience with CO2 capture from coal flue gas in pilot-scale: Testing of different amine solvents. Energy Procedia 1: 783–790.

Kohl A & Nielsen L (1997) Gas purification. 5th edition. Houston: Gulf professional publishing.

Konduru P, Vaidya P & Kenig E (2010) Kinetics of Removal of Carbon Dioxide by Aqueous Solutions of N,N- Diethylethanolamine and Piperazine. Environmental Science & Technology 44 (6): 2138-2143.

Kothandamaran A (2010) Carbon dioxide capture by chemical absorption: A solvent comparison study. PhD dissertation. Massachusetts: Massachusetts Institute of Technology.

Kroon (2013) Separation technology group: CO_2 capture with novel nature based solvents. http://www.tue.nl/fileadmin/content/faculteiten/st/Onderzoek/Onderzoeksgroepen/Separation_Technology/Totaal_Japiebundel_2013.pdf. [15.11.2013].

Lepaumier H, Picq D & Carrette P-L (2009a) New Amines for CO_2 Capture I. Mechanisms of Amine Degradation in the Presence of CO_2. Industrial & Engineering Chemistry Research 48 (20): 9061–9067.

Lepaumier H, Picq D & Carrette P-L (2009b) New Amines for CO_2 Capture II. Oxidative Degradation Mechanisms. Industrial & Engineering Chemistry Research 48 (20): 9068–9075.

Liebenthal U (2011a) Integration of post-combustion CO_2 capture processes into coal-fired steam power plants. http://www.icapco2.org/0/17/eu-ccs-workshop-china/. [15.2.2014].

Liebenthal U, Linnenberg S, Oexmann J & Kather A (2011b) Derivation of correlations to evaluate the impact of retrofitted post-combustion CO_2 capture processes on steam power plant performance. International Journal of Greenhouse Gas Control 5 (5): 1232-1239.

Liebenthal U, Pinto D, Monteiro J, Svendsen H & Kather A (2013) Overall Process Analysis and Optimisation for CO_2 Capture from Coal Fired Power Plants based on Phase Change Solvents Forming Two Liquid Phases. Energy Procedia 37: 1844-1854.

Majeed H (2013) Reactive absorption of CO_2 in single and blended amine systems. Thesis, Norwegian University of Science and Technology.

McCann N, Maeder M & Attalla M (2008) Simulation of enthalpy and capacity of CO_2 absorption by aqueous amine systems. Industrial & Engineering Chemistry Research 47: 2002-2009.

Mikunda T (2012) CO_2 storage: do impurities matter? http://www.globalccsinstitute.com/insights/authors/tommikunda/2012/01/18/co2-storage-do-impurities-matter. [24.10.2013].

Mitch W (2013) Task report 1: Predicted products of solvent decay and experimental plan. http://www.gassnova.no/no/Documents/Predictedproductsofsolventdecayandexperimentalplan_Yale.pdf. [17.1.2014].

Monteiro J, Pinto D & Svendsen H (2011) Phase change solvents. EU-China workshop on innovative CCs technologies. Beijing: iCap.

Monteiro J, Pinto D, Zaidy S, Hartono A & Svendsen F (2013) VLE data and modelling of aqueous N,N-diethylethanolamine (DEEA) solutions. International Journal of Greenhouse Gas Control 19: 432–440.

Mustonen S (2013) Carbon dioxide recovery with activated methyldiethanolamine. Master's thesis. University of Oulu.

Onarheim K (2012) Carbon capture solvent screening. Espoo: VTT.

Perry R, Wood B, Genovese S, O'Brien M, Westendorf T, Meketa M, Farnum R, McDermott J, Sultanova I, Perry T, Vipperla R-K, Wichmann L, Enick R, Hong L & Tapriyal D (2012) CO_2 capture using phase-changing sorbents. Energy & Fuels 26 (4): 2528-2538.

Pinto D, Monteiro J, Bruder P, Zaidy S, Jonassen Ø, Hartono A & Svendsen H (2011) Correlation and Prediction of Vapor-Liquid-Liquid Equilibrium using the e-NRTL model applied to the MAPA-DEEA-CO_2-Water System. Trondheim.

Pinto D, Monteiro J, Knuutila H, Tobiesen F, Mejdell T & Svendsen H (2013) Simulation of a Phase Change System for CO_2 Capture. https://aiche.confex.com/aiche/2013/webprogram/Paper334286.html. [15.1.2013].

Pinto D, Knuutila H, Monteiro J & Svendsen H (2014) Pilot campaign for phase change solvents. icapco2.org/files/11u20_Di_Domenico_iCap_Pilot_Campaign_v3.pdf. [5.2.2014].

Purarelli (1994) Separators, liquid-vapor, horizontal design. McKetta (Ed.) Encyclopedia of chemical processing and design, Volume 49 : Safety, OSHA compliance to separators, vertical, sizing with computers. New York, Dekker: 469-476.

Puxty G, Rowland R, Allport A, Yang Q, Bown M, Burns M, Maeder M & Attalla M (2009) Carbon dioxide post-combustion capture: Anovel screening study of the carbon dioxide absorption performance of 76 amines. Environmental Science & Technology 43: 6427-6433.

Raynal L, Alix P, Bouillon P-A, Gomez A, le Febvre de Nailly M, Jacquin M, Kittel J, Lell A, Mougin P & Trapy J (2011) The DMX™ process : an original solution for lowering the cost of post-combustion carbon capture. Energy Procedia 4: 779–786.

Rochelle G (2009) Amine scrubbing for CO_2 capture. Science 235: 1652-1654.

Rochelle G, Freeman S, Voice A & Closmann F (2011) Degradation of amines in CO_2 capture. https://www.sintef.no/project/TCCS6/Presentations/A3/02_15%2040%20%20%20A3%202%20rochelle%20deg%20review%20trondheim%20final.pdf. [12.2.2014].

Rojey A, Cadours R, Carrette P & Boucot P (2009) Method of deacidizing a gas by means of an absorbent solution with fractionated regeneration through heating. Patent. US 2009/0199709 A1.

Sartori G & Savage D (1983) Sterically hindered amines for CO_2 removal from gases. Industrial & Engineering Chemistry Fundamentals 22 (2): 239-249.

Selker A & Schleicher C (1965) Factors affecting which phase will disperse when immiscible liquids are stirred together. The Canadian Journal of Chemical Engineering 43: 298–301.

Sigma-Aldrich (2014a) 2-(Diethylamino)ethanol. http://www.sigmaaldrich.com/catalog/product/aldrich/471321?lang=fi&region=FI. [10.2.2014].

Sigma-Aldrich (2013b) 2- (Dimethylamino)-1-propylamine. http://www.sigmaaldrich.com/catalog/product/aldrich/240052?lang=fi&region=FI. [10.2.2014].

Sinnott R (2005) Chemical engineering design: Principles, practice and economics of plant and process design. Jordan-Hill: Butterworth-Heinemann.

Speight J (1999) Desulfurization of Heavy Oils and Residual. 2nd Edition. New York: CRC Press.

Spellman F & Whiting N (2005) Environmental engineer's mathematics handbook: Chapter 9: Particulate emission control. CRC Press LLC.

Suvanto J (2013) Emissions of carbon dioxide capture in power generation when using precombustion capture or oxyfuel combustion methods. Master's thesis. Tampere University of Technology.

Svendsen H (2012) Phase change solvents; can they deliver? http://www.sintef.no/project/NORDICCS/Presentations%20Technoport/Phase%20change%20solvents%20Technoport%202012%20%5BCompatibility%20Mode%5D.pdf. [13.1.2014].

Thomsen K (2013) Current status of R&D in post combustion CO_2 capture. https://www.chalmers.se/en/areas-of-advance/energy/Documents/Chalmers%20Energy%20Conference%202011/KajThomsen%20PCCC.pdf. [29.1.2014].

U.S. Environmental protection agency (2013a) Flue Gas Desulfurization (Acid gas recovery system). http://yosemite.epa.gov/oaqps/EOGtrain.nsf/DisplayView/SI_412C_9?OpenDocument. [24.10.2013].

U.S. Environmental protection agency (2013b) Natural gas processing. http://www.epa.gov/ttnchie1/ap42/ch05/final/c05s03.pdf. [28.1.2014].

Uusi-Kyyny P (2014) Initial experiments involving phase change solvents: MAPA and DEEA with CO_2, density and viscosity. Report, 24.2.2014. Aalto University, Department of Biotechnology and Chemical Technology. Asked permission.

Voice A, Vevelstad S, Chen X, Nguyen T, Rochelle G (2013) Aqueous 3-(methylamino)propylamine for CO_2 capture. International Journal of Greenhouse Gas Control 15: 70–77.

Wang M, Lawal A, Stephenson P, Sidders J, Ramshaw C & Yeung H (2011) Post-combustion CO_2 Capture with Chemical Absorption: A State-of-the-art Review. Chemical Engineering Research and Design 89 (9): 1609-1624.

Xu Z, Wang S, Qi G, Liu J, Zhao B & Chen C (2013) CO_2 absorption by biphasic solvents: Comparison with lower phase alone. Oil & Gas Science and Technology.

Yeh A & Bai H (1999) Comparison of ammonia and monoethanolamine solvents to reduce CO_2 greenhouse gas emissions. The Science of the Total Environment 228: 121-133.

Zhang J, Nwani O & Agar D (2010) Carbon dioxide absorption into biphasic amine solvent with solvent loss reduction. de Haan A, Kooijman H & Górak (Eds.) Distillation absorption 2010: 169-174.

Zhang J, Agar W, Zhang X & Geuzebroek F (2011a) CO_2 absorption in biphasic solvents with enhanced low temperature solvent regeneration. Energy procedia 4: 67-74.

Zhang J, Onyekachi N & Agar D (2011b) Carbon dioxide absorption into biphasic amine solvent with solvent loss reduction. Chemical Engineering Research & Design: Transactions of the Institution of Chemical Engineers, Part A 89 (8): 1190-1196.

Zubeir L, Francisco M, Peters C & Kroon M (2013) Deep eutectic solvents as promising alternative for the current CO_2 capture solvents. http://www.eventure-online.com/eventure/publicAbstractView.do?id=206694&congressId=6293. [2.1.2014].

15 APPENDICES

Appendix 1. Reboiler duties. (Table 14.)

Appendix 2. Figures 7 and 8 of the decanter dimensions.

Appendix 3. Tables 15-22 of the calculations of the experimental part of the thesis.

Appendix 1. Reboiler duties.

Table 14. Reboiler duties for MEA, MDEA+PZ and DEEA + MAPA systems for recovered CO$_2$.

		Regeneration temperature [°C]	Regeneration pressure [kPa]	Reboiler duty [MJ/kg]	CO$_2$ recovery [%]	CO$_2$ molefrac in lean from stripper	Reference
MEA	30 wt-%						
CO2SIM		120	300	3.1		0.24	Aroonwilas et al. 2007
		120	200	3.2	90		Liebenthal et al. 2013
			190	3.7	88		Knudsen 2007
			190	4.2	85-95		Chapel et al. 1999
		125	170	4.25	85	0.20-0.28	Kothandamaran, 2010
				4.8		0.18	Aroonwilas et al. 2007
MDEA+PZ	ratio in kmol/m^3						
Aspen Plus, closed amine circulation	0.365 PZ /2.635 MDEA	120	202.65	4.06	84.50	0.0219	Mustonen 2013
	0.6 PZ / 4.0 MDEA	120	202.65	3.89	88.02	0.0165	Mustonen 2013
Aspen Plus, removal of heat stable salts	0.365 PZ /2.635 MDEA	120	202.65	3.90	87.96	0.0170	Mustonen 2013
	0.6 PZ / 4.0 MDEA	120	202.65	3.82	89.71	0.0146	Mustonen 2013
DEEA+MAPA	5M DEEA / 2M MAPA						
CO2SIM		88	400	2.4	90		Liebenthal et al. 2013
Pilot plant		107-117	175 (abs)	2.52-7.74			Pinto et al. 2014
LabPilot		141.96	400	2.19917	82.37	0.0375	Svendsen 2012
LabPilot		149.38	600	2.24408	80.68	0.0409	Svendsen 2012
LabPilot		155.49	600	2.24896	87.24	0.0274	Svendsen 2012

Appendix 2. Figures 7 and 8 of the decanter dimensions.

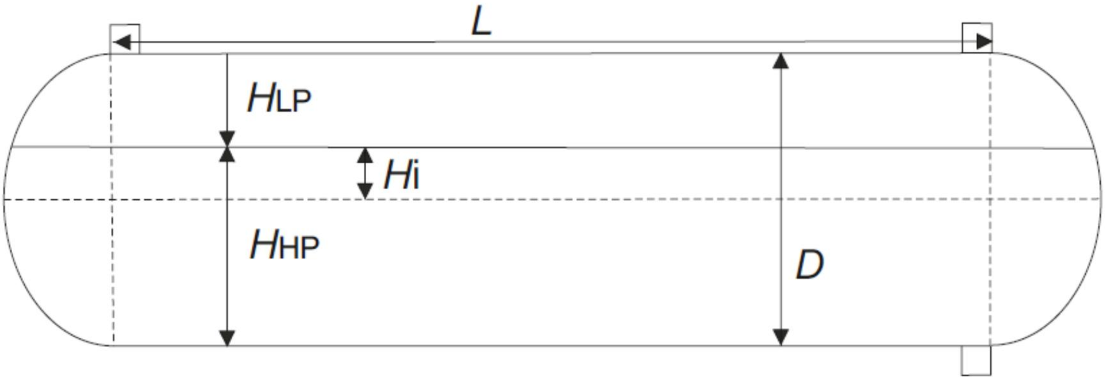

Figure 7. Decanter dimensions.

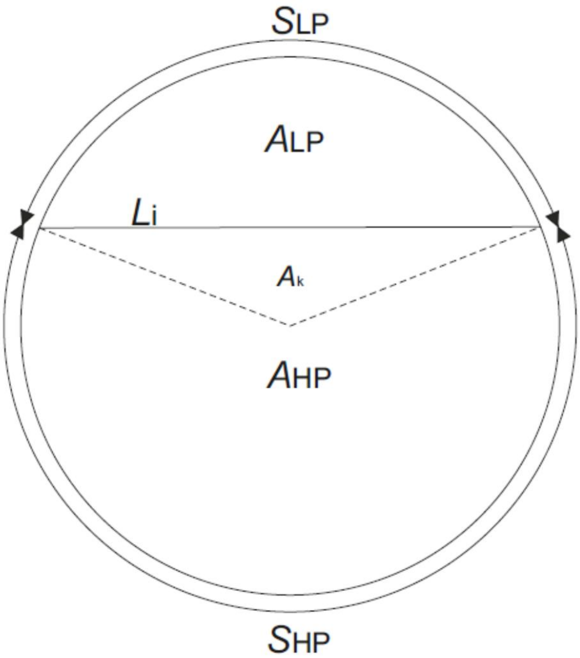

Figure 8. Cross-section of the decanter.

Appendix 3. Tables 16-23 of the calculations of the experimental part of the thesis.

Table 15. The solvent flows for different cases of absorbed carbon dioxide.

Case 1	DEEA	MAPA	H_2O	SOLVENT
Concentration *w* [mass fraction]	0.635	0.191	0.174	1
Concentration *x* [mole fraction] (Eq. 27)	0.314	0.126	0.560	1
Molar mass *M* [g/mol]	117.19	88.15	18.015	94.39
Molar flow *N* [mol/s] (Eqs. 18, 25)	13770		17534	31304
Mass flow *m* [g/s] (Eqs. 26, 28)	1152782	346742	315880	1815404
Mass flow *m* [kg/h]	4150014	1248272	1137169	6535455
L/G ratio [kg/m^3] (Eq. 19)	-	-	-	3.474
Loading of CO_2 [mol CO_2/mol amine]	-	-	-	0.196
Case 2	DEEA	MAPA	H_2O	SOLVENT
Concentration *w* [mass fraction]	0.635	0.191	0.174	1
Concentration *x* [mole fraction] (Eq. 27)	0.314	0.126	0.560	1
Molar mass *M* [g/mol]	117.19	88.15	18.015	94.39
Molar flow *N* [mol/s] (Eqs. 18, 25)	5998		7637	13635
Mass flow *m* [g/s] (Eqs. 26, 28)	502100	151025	137583	790709
Mass flow *m* [kg/h]	1807562	543692	495300	2846554
L/G ratio [kg/m^3] (Eq. 19)	-	-	-	1.513
Loading of CO_2 [mol CO_2/mol amine]	-	-	-	0.45
Case 3	DEEA	MAPA	H_2O	SOLVENT
Concentration *w* [mass fraction]	0.635	0.191	0.174	1
Concentration *x* [mole fraction] (Eq. 27)	0.314	0.126	0.560	1
Molar mass *M* [g/mol]	117.19	88.15	18.015	94.39
Molar flow *N* [mol/s] (Eqs. 18, 25)	2699		3437	6135
Mass flow *m* [g/s] (Eqs. 26, 28)	225945	67961	61913	355819
Mass flow *m* [kg/h]	813403	244661	222885	1280949
L/G ratio [kg/m^3] (Eq. 19)	-	-	-	0.681
Loading of CO_2 [mol CO_2/mol amine]	-	-	-	1
Case 4	DEEA	MAPA	H_2O	SOLVENT
Concentration *w* [mass fraction]	0.635	0.191	0.174	1
Concentration *x* [mole fraction] (Eq. 27)	0.314	0.126	0.560	1
Molar mass *M* [g/mol]	117.19	88.15	18.015	94.39
Molar flow *N* [mol/s] (Eqs. 18, 25)	145		185	330
Mass flow *m* [g/s] (Eqs. 26, 28)	12168	3660	3334	19162
Mass flow *m* [kg/h]	43804	13176	12003	68982
L/G ratio [kg/m^3] (Eq. 19)	-	-	-	0.037
Loading of CO_2 [mol CO_2/mol amine]	-	-	-	18.57

Table 16. General data for decanter calculations.

Density of the light phase (Uusi-Kyyny, 2014)	ρ_{LP} [kg/m^3]	928.17
Density of the heavy phase (Uusi-Kyyny, 2014)	ρ_{HP} [kg/m^3]	1114.38
Viscosity of the light phase (Uusi-Kyyny, 2014)	μ_{LP} [cP]	12.6
Viscosity of the heavy phase (Uusi-Kyyny, 2014)	μ_{HP} [cP]	1480
Gravitational acceleration	g [m/s^2]	9.81
Droplet diameter	d [m]	0.00100

Table 17. Dispersion factor calculated with the Equations (20) and (32).

		Case 1	Case 2
Dispersion factor (Eq. 32)	c	7.9	4.9
Volumetric flow rate of the light phase (Eq. 20)	Q_{LP} [m^3/s]	1.3	0.5
Volumetric flow rate of the heavy phase (Eq. 20)	Q_{HP} [m^3/s]	0.7	0.4

Table 18. Dimensions of the vessel that are calculated with the Equations (33)-(42).

		Case 1	Case 2
The chosen diameter	D [m]	7.8	4.4
The chosen length	L [m]	25.1	17.8
Radius	r [m]	3.9	2.2
Length to dimension ratio	L/D	3.2	4.0
Volume of the vessel (Eq. 33)	V_{TOT}	1199.4	270.7
The distance of the interphase from the middle	H_i	-1.3	-0.2
The width of the interface (Eq. 34)	L_i	7.4	4.4
Surface of the interface (Eq. 35)	A_i	184.6	77.8
The distance of the interface from the bottom (Eq. 36)	H_{HP}	2.6	2.0
The height of the light phase (Eq. 37)	H_{LP}	5.2	2.4
The cross-sectional surface area of the vessel (Eq.38)	A [m^2]	47.8	15.2
The cross-sectional surface area of the light phase (Eq. 39)	$A_{LP}=A_{sector}-A_k$	33.8	8.7
The cross-sectional surface area of the heavy phase (Eq. 40)	$A_{HP}=A-A_{LP}$	13.9	6.5
Volume of the light phase (Eq. 41)	V_{LP} [m^3]	849.4	154.5
Volume of the heavy phase (Eq. 42)	V_{HP} [m^3]	350.0	116.2

Table 19. Settling velocity calculated with the Equation (43).

As the heavy phase is disperged:		Case 1	Case 2
The falling velocity of the heavy phase drops (Eq. 43)	$V_{d,HP}$ [m/s]	0.0081	0.0081

Table 20. Reynolds number calculated with the Equations (49)-(51).

		Case 1	Case 2
The length of the arc of the sector of light phase (Eq. 50)	$S_{LP,segment}$ [m]	14.9	7.4
Hydraulic diameter of the heavy phase (Eq. 51)	$D_h=4A_{HP}/\text{perimeter}_{HP}$ [m]	3.3	2.4
Reynolds number (Eq. 49)	Re	116.6	113.5

Table 21. Vapour pressures and partial pressures of the solvent in the stripper conditions calculated with the Equations (54) and (55).

Ciftja et al. 2013c [mol]		Mole fraction x
DEEA	0.2	0.12
MAPA	0.8	0.54
WATER	0.5	0.34

Temperature	Vapour pressures P^o [kPa]			Partial pressures p [kPa]			
T [°C]	DEEA (Hartono 2013)	MAPA (Hartono 2013)	Water (Haar et al. 1984)	DEEA (Eq. 54)	MAPA (Eq. 54)	Water (Eq. 54)	Total (Eq. 55)
88.00	8.42	16.85	70.12	8.69	37.77	23.66	70.12
107.00	236.34	420.40	101.32	12.55	54.58	34.18	101.32
141.96	483.28	853.61	143.24	17.75	77.16	48.33	143.24
149.38	553.97	977.90	198.48	24.59	106.92	66.97	198.48
155.49	617.68	1090.04	270.02	33.46	145.46	91.10	270.02

Table 22. The partial pressures of the solvent and carbon dioxide in the stripper calculated with the Equations (54) and (55) and the volume flow of the gas phase from the stripper calculated with the Equation (53).

	Partial pressure of the solvent (Eq. 55) p_{TOT} [kPa]	Partial pressure of CO_2 (Eq. 54) p_{CO2} [kPa]	Volume flow of the gas phase from the stripper (Eq. 53) Q_{gas} [m^3]
1	70	329.88	1.8
2	101	73.68	-
3	143	256.76	2.1
4	198	401.52	0.9
5	270	329.98	1.2